Figure 16 Results from NRM magnetic intensity measurements for the basalt specimens from the anomalies A, G, JF5 and Q. The depths of the specimens for the different anomalies are noted in the box panels near the top.

Saurav Biswas
March 5, 2007
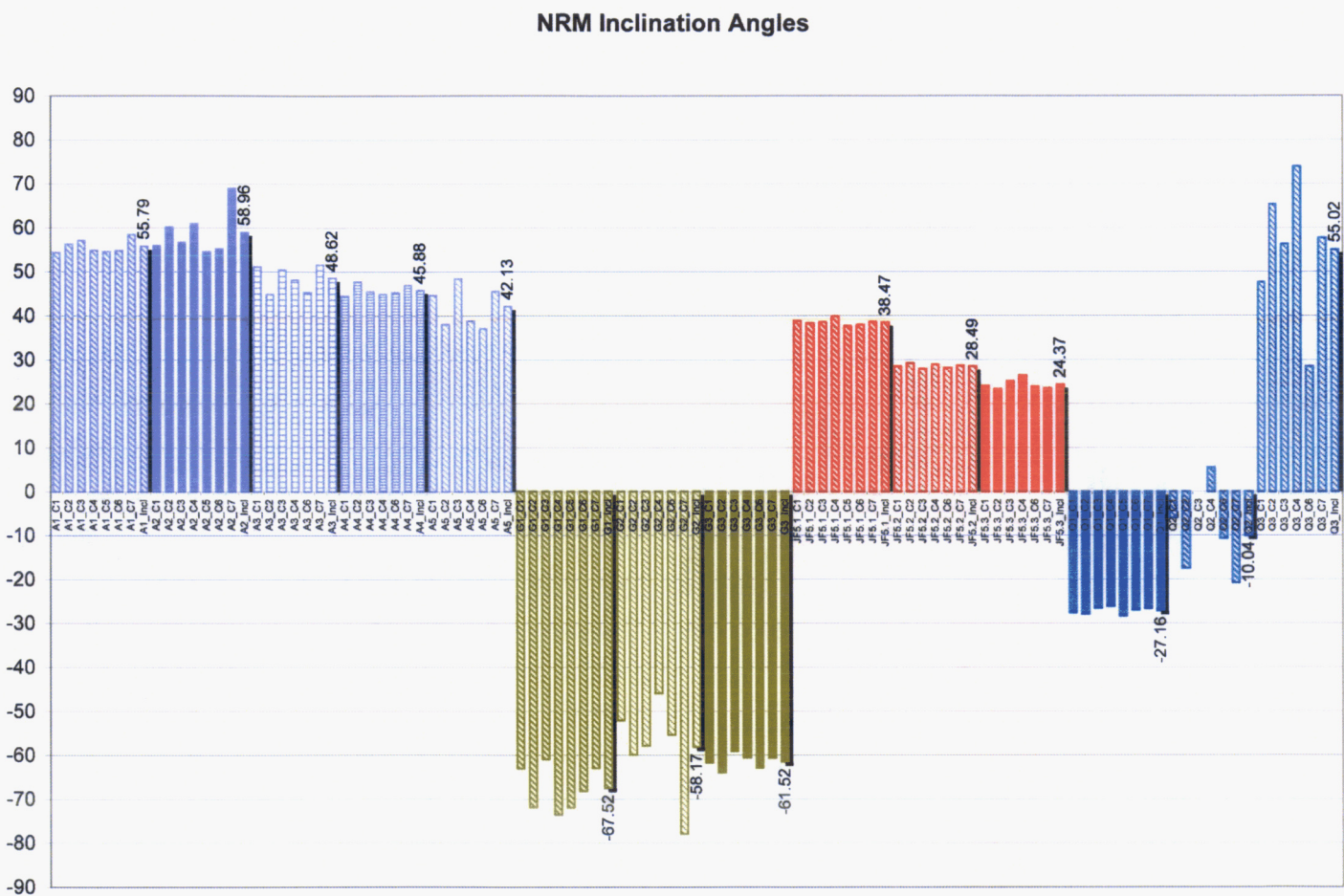
Scientific Notebook 758E

NRM Inclination Angles

Figure 17 Results from inclination only statistics of NRM magnetic intensities for the basalt specimens from the anomalies A, G, JF5 and Q.
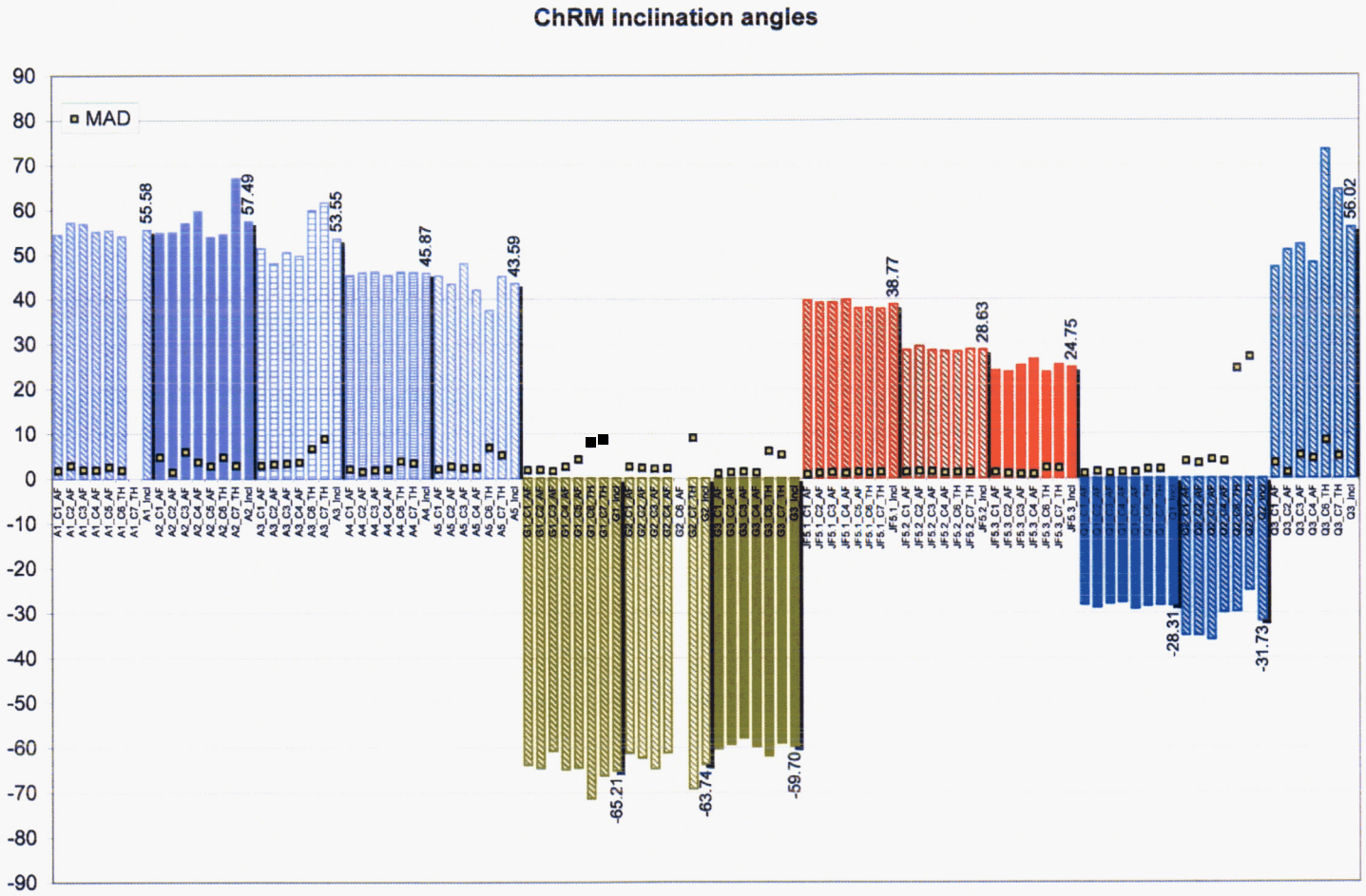
ChRM inclination angles

Figure 18 Results from inclination only statistics of ChRM magnetic intensities for the basalt specimens from the anomalies A, G, JF5 and Q. MAD - Mean Angular Deviation.
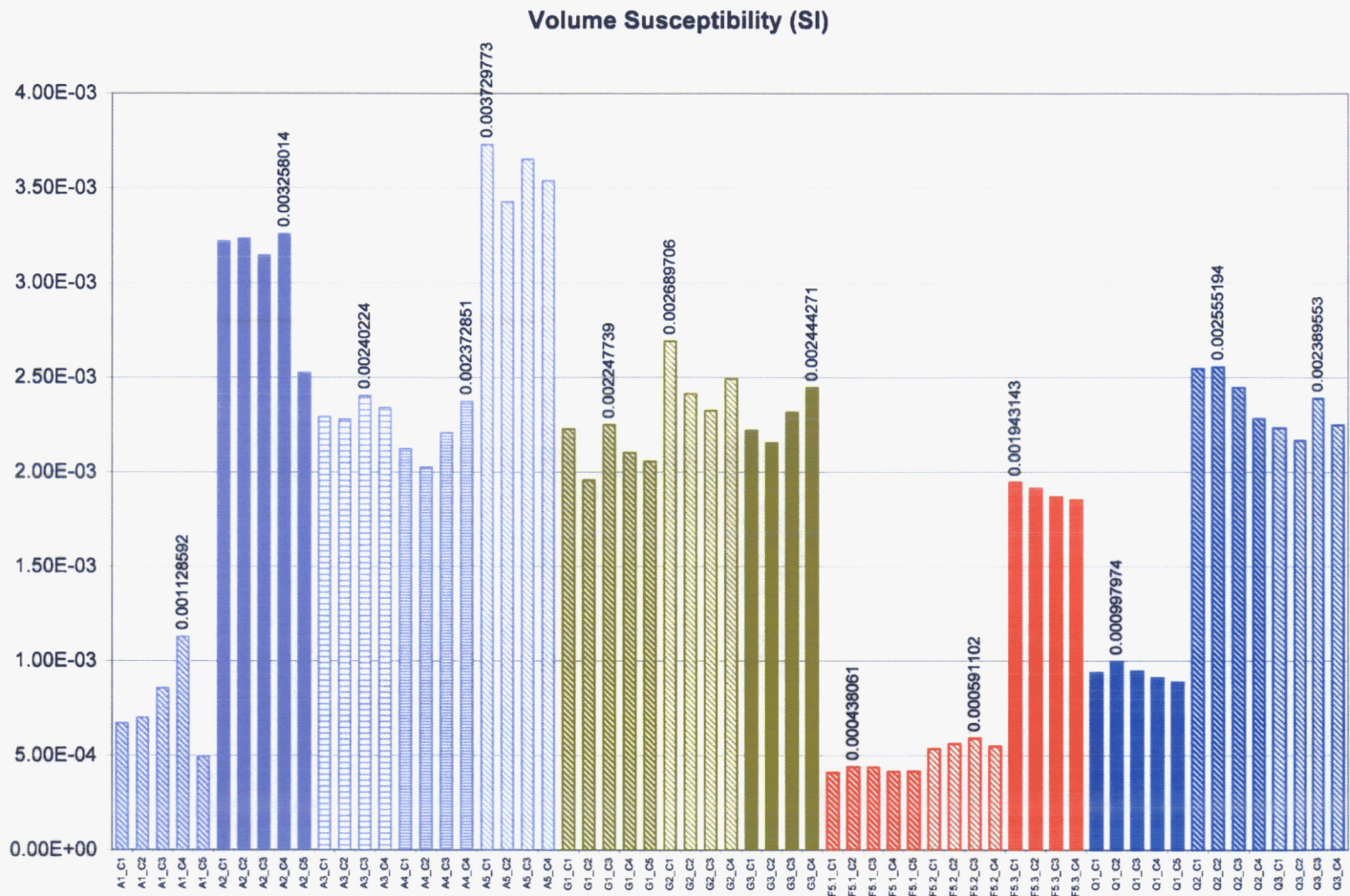
Figure 19 Results from volume susceptibility measurements for the basalt specimens from the anomalies A, G, JF5 and Q.
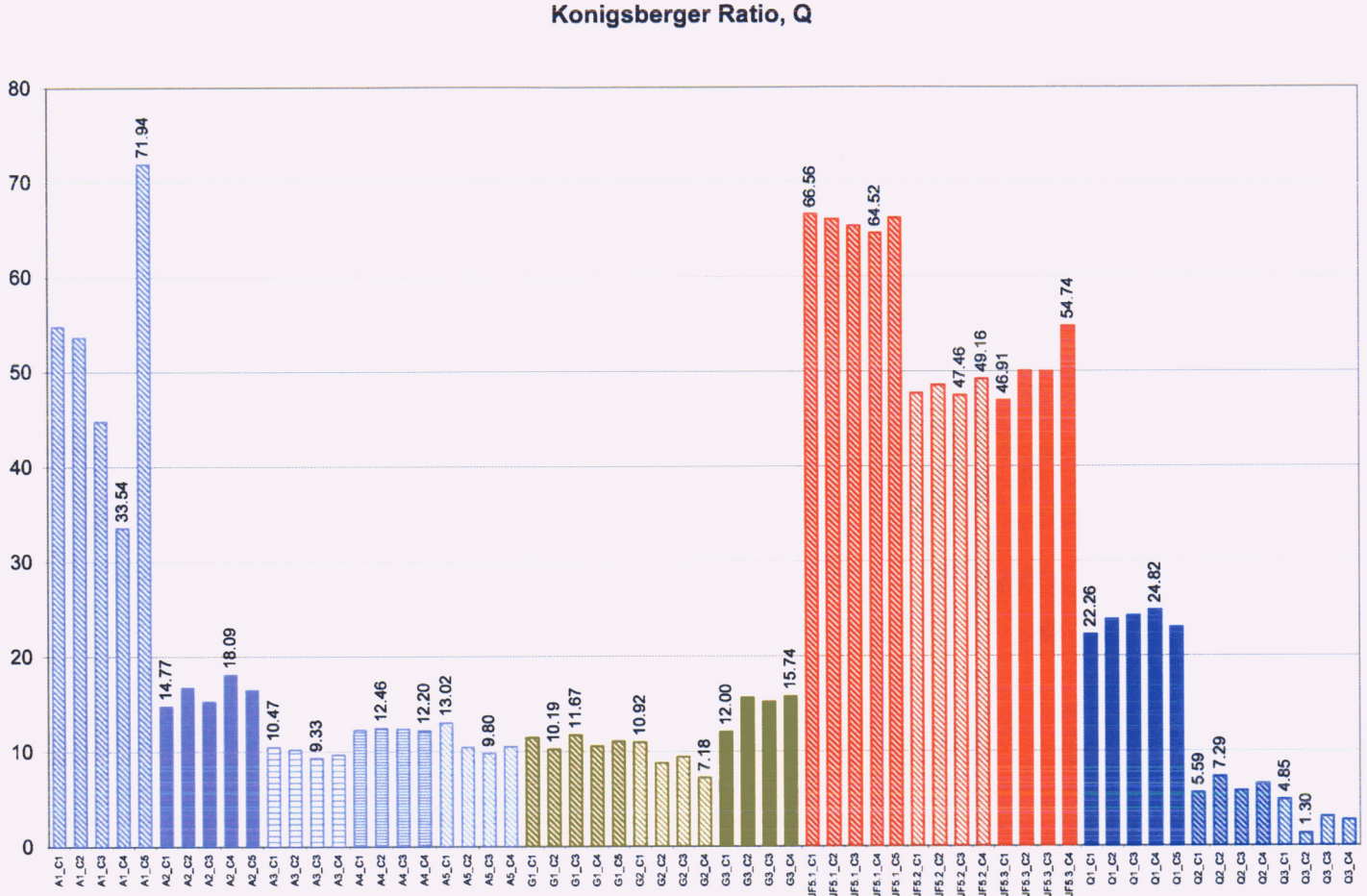
Figure 20 Results of Konigsberger ratio (Q) for the basalt specimens from the anomalies A, G, JF5 and Q.
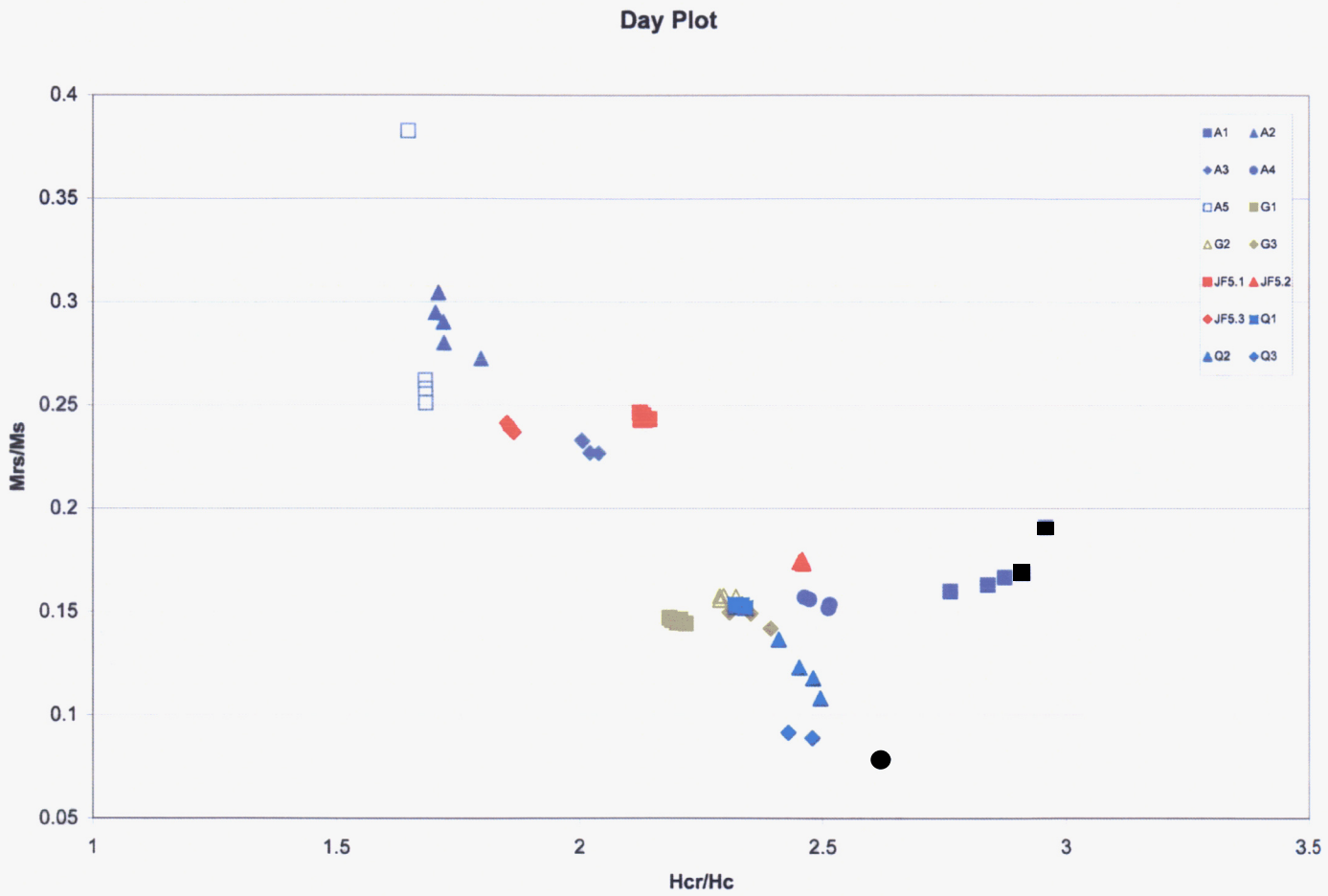
Day Plot

Figure 21 Results of Day plot from hysteresis and coercivity measurements of the basalt specimens from the anomalies A, G, JF5 and Q.

Entry: Saurav Biswas
Date: March 5, 2007
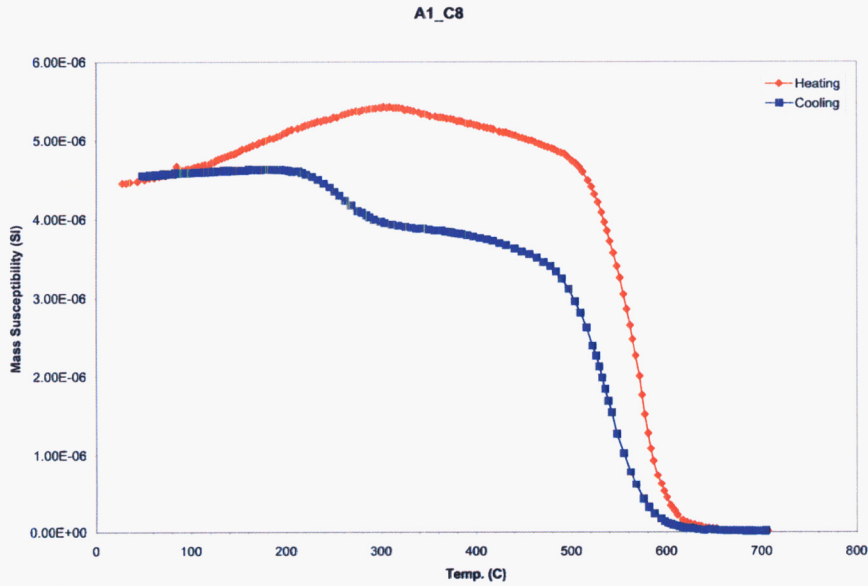
A1_C8

Figure 22 Results from high temperature susceptibility measurements for specimen A1_C8.

A2_C8

Figure 23 Results from high temperature susceptibility measurements for specimen A2_C8.

Entry: Saurav Biswas
Date: March 5, 2007

A3_C8

Figure 24 Results from high temperature susceptibility measurements for specimen A3_C8.

A4_C8

Figure 25 Results from high temperature susceptibility measurements for specimen A4_C8.

Entry: Saurav Biswas

Date: March 5, 2007

Figure 26 Results from high temperature susceptibility measurements for specimen A5_C8.

Entry: Saurav Biswas
Date: March 5, 2007

Figure 27 Results from high temperature susceptibility measurements for specimen G1_C8.
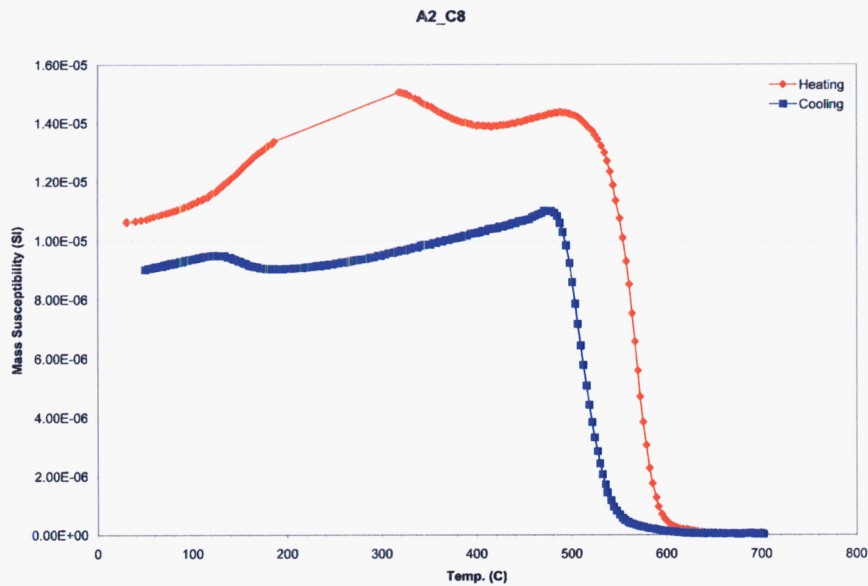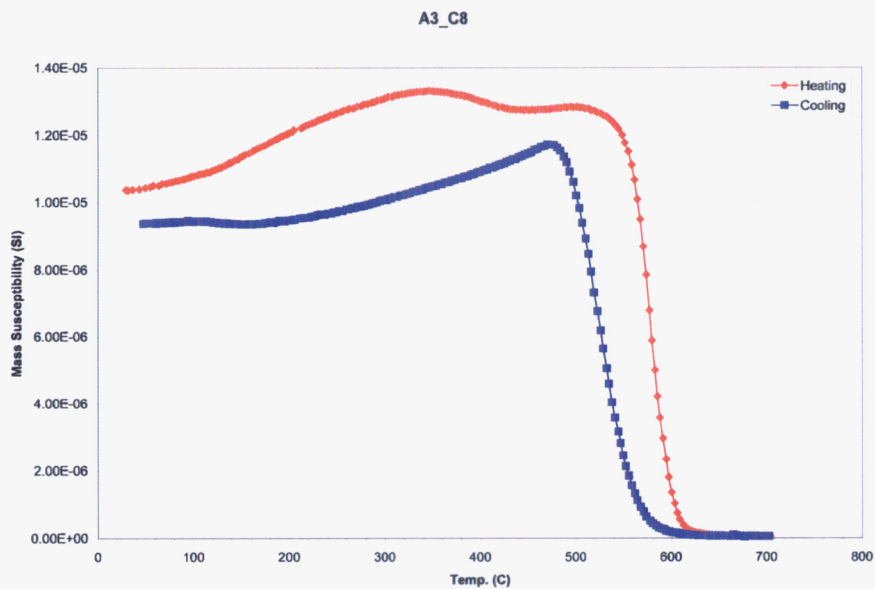
Figure 28 Results from high temperature susceptibility measurements for specimen G2_C8.

Entry: Saurav Biswas
Date: March 5, 2007
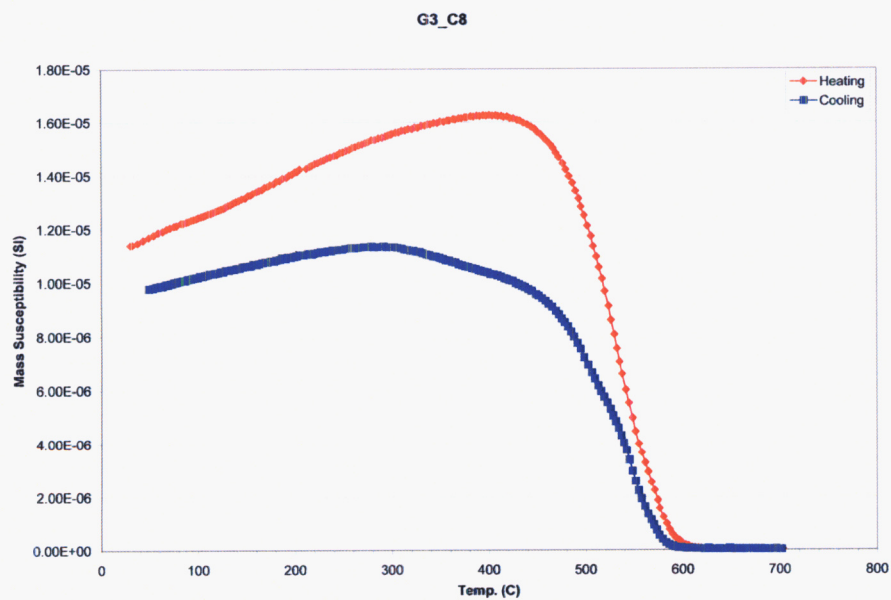
G3_C8

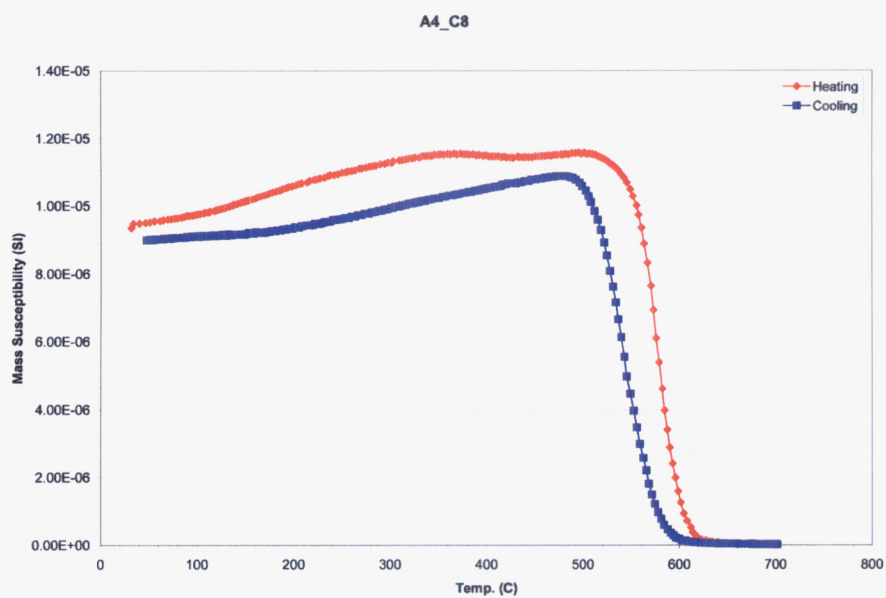**Figure 29** Results from high temperature susceptibility measurements for specimen G3_C8.

Entry: Saurav Biswas
Date: March 5, 2007
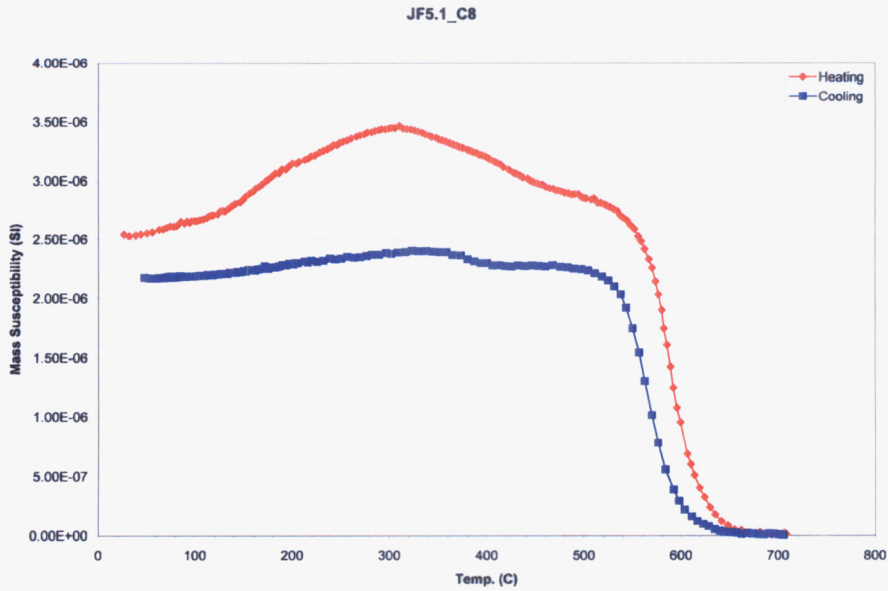
JF5.1_C8

Figure 30 Results from high temperature susceptibility measurements for specimen JF5.1_C8.
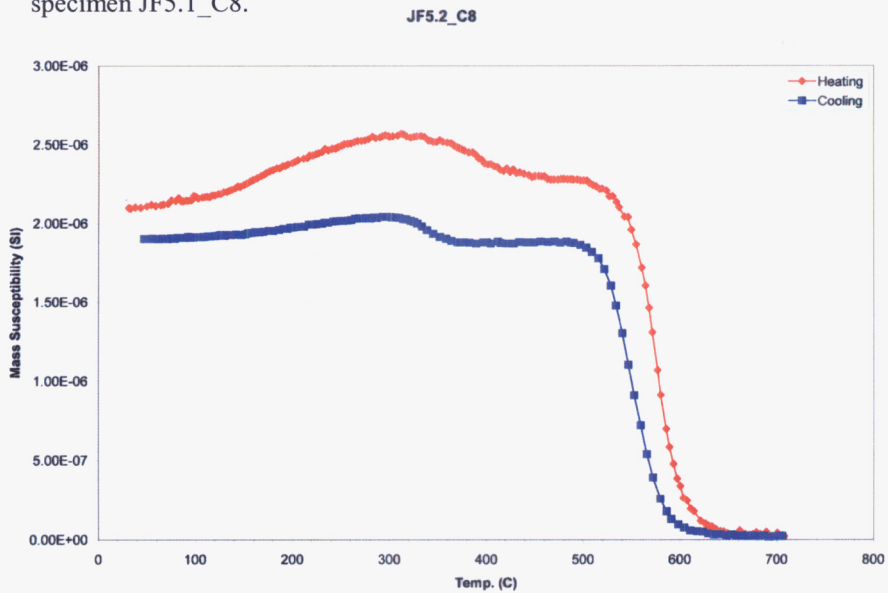
JF5.2_C8

Figure 31 Results from high temperature susceptibility measurements for specimen JF5.2_C8.
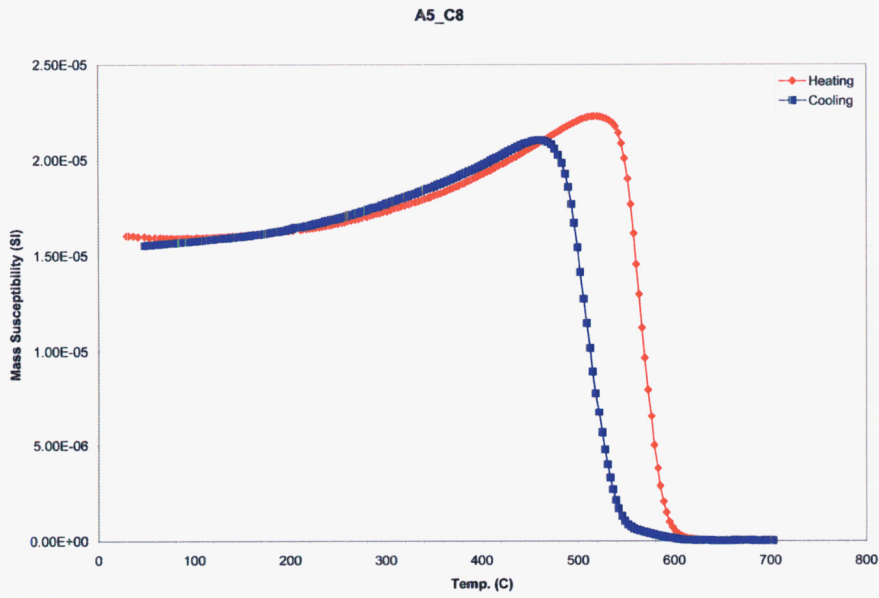
Entry: Saurav Biswas
Date: March 5, 2007
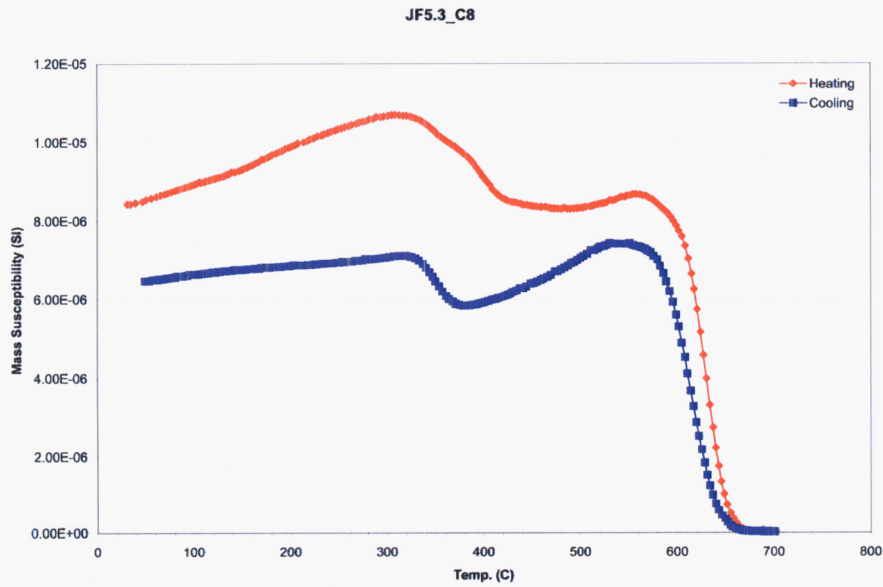
Figure 32 Results from high temperature susceptibility measurements for specimen JF5.3_C8.

Entry: Saurav Biswas
Date: March 5, 2007
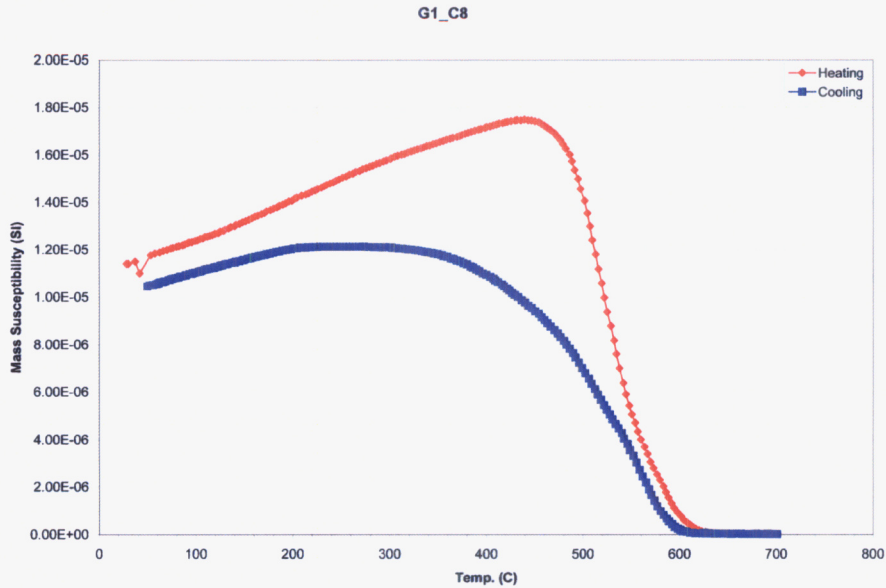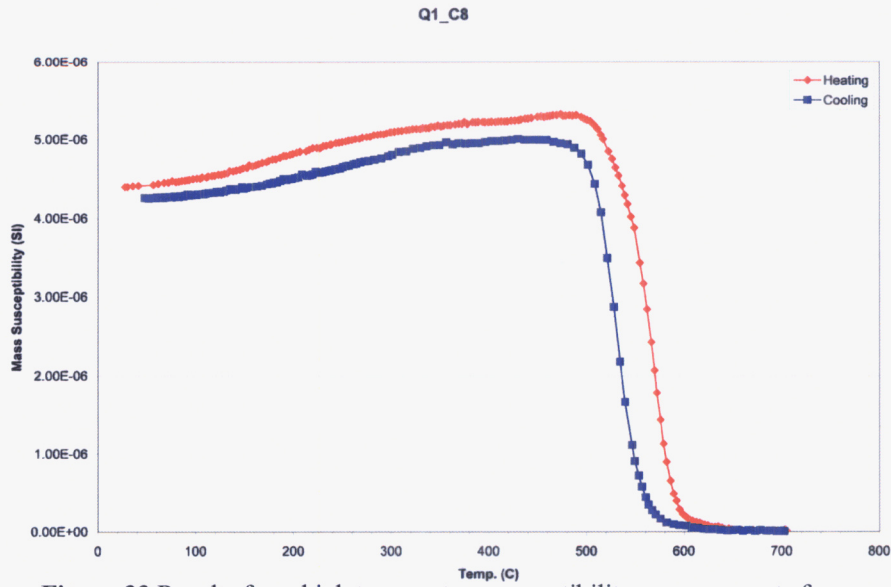
Q1_C8

Figure 33 Results from high temperature susceptibility measurements for specimen Q1_C8.
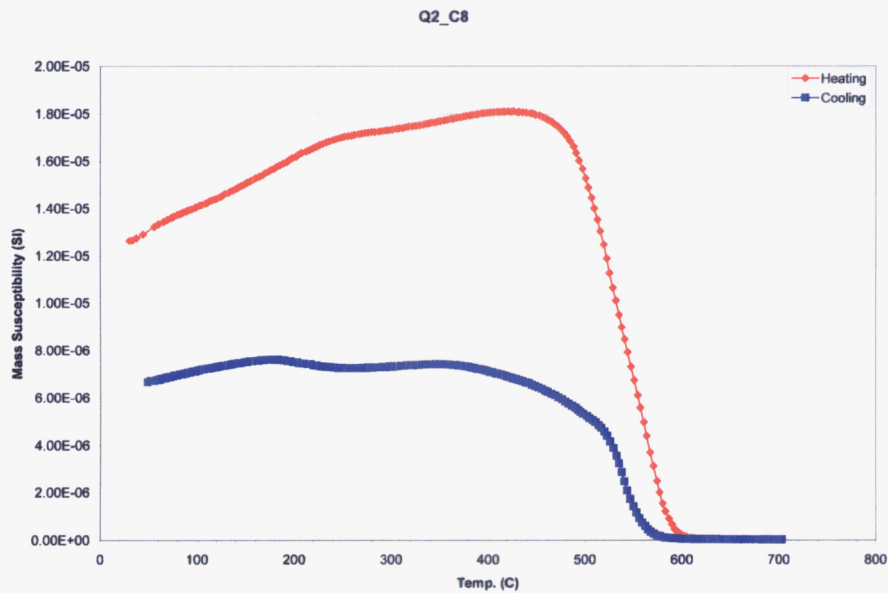
Q2_C8

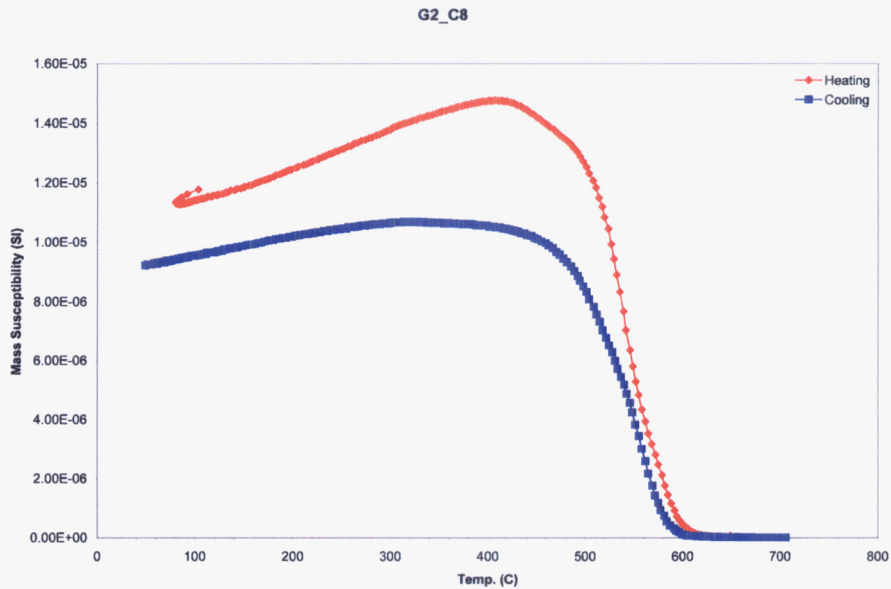**Figure 34** Results from high temperature susceptibility measurements for specimen Q2_C8.

Entry: Saurav Biswas
Date: March 5, 2007
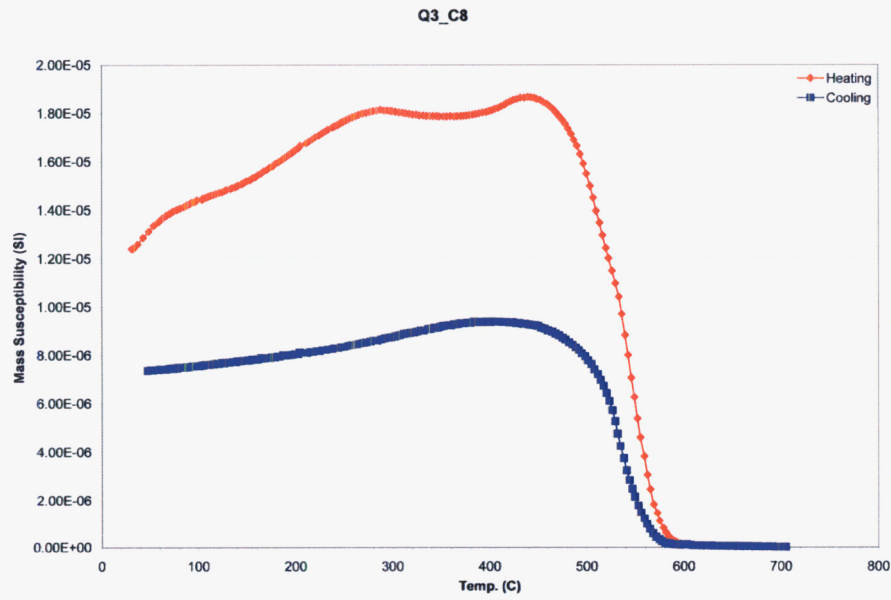
Q3_C8

Figure 35 Results from high temperature susceptibility measurements for specimen Q3_C8.

Ordering Temperature
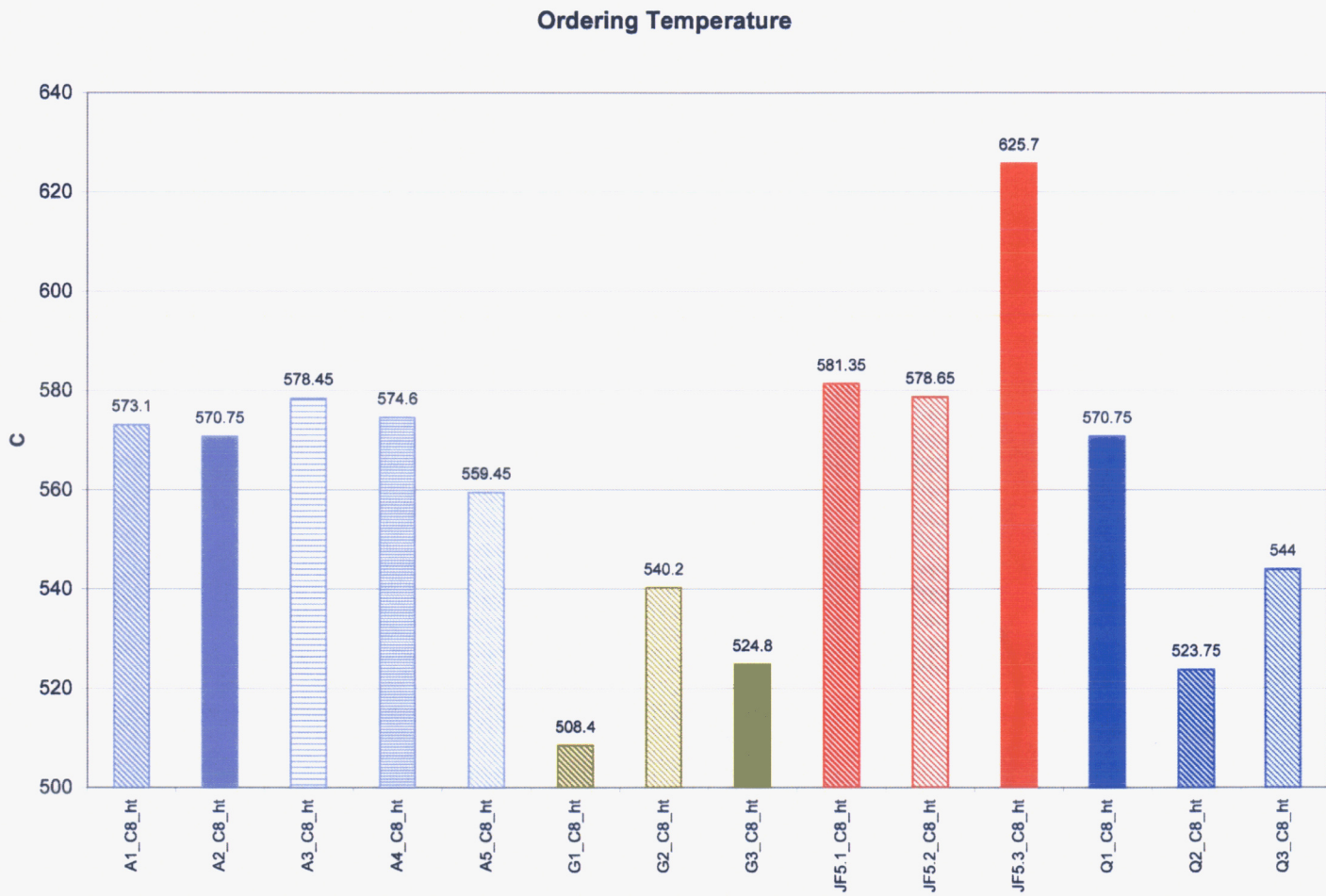
Figure 36 Ordering temperatures of the basalt specimens from anomalies A, G, JF5 and Q determined from the high temperature susceptibility measurements.

Scientific Notebook 758E

Entry: Saurav Biswas
Date: March 5, 2007

Reference:

McFadden, P.L., and Reid, A.B. "Analysis of paleomagnetic inclination data" Geophys. J. R. astr. Soc. (1982) 69, 307-319.

Spivey K.H., and Stamatakos, J.S. "Field trip to review the structural and volcanic geology of Death Valley, CA and its relative similarities to the Yucca Mountain Region" (12/02/1993 through 05/162000), Scientific Notebook No. 099, 59-62p.

Dunlop, D.J., and Ö. Özdemir, *Rock Magnetism: Fundamentals and Frontiers*, 573 pp., Cambridge University Press, Cambridge, 1997.

Evans, M.E., and F. Heller, *Environmental Magnetism: Principles and Applications of Environmagnetics*, Academic Press, Elsevier Science, Amsterdam, 2003.

Entry: Saurav Biswas
Date: March 7, 2007

Entry 10. Locations of anomalies A, G, JF5 and Q and the corresponding boreholes on the aeromagnetic anomaly map and 2D models of the associated profiles for anomalies G and JF5.

Figure 37 Total field aeromagnetic anomaly map around Yucca Mountain, Nevada compiled at approximately 30 m above the ground surface. The white rectangles show the anomalies A, G, JF5 and Q.

52

Entry: Saurav Biswas
Date: March 7, 2007

Table 8 Location of anomaly boreholes and depth of basalt intercept

Anomaly	Easting (m)	Northing (m)	Depth of basalt intercept (m)
A	534869.48	4067574.61	154.3
G	546133.10	4054714.10	130.1
JF5	557845.94	4069543.07	83.3
Q	538165.10	4077678.50	147.6

Entry: Saurav Biswas
Date: March 7, 2007

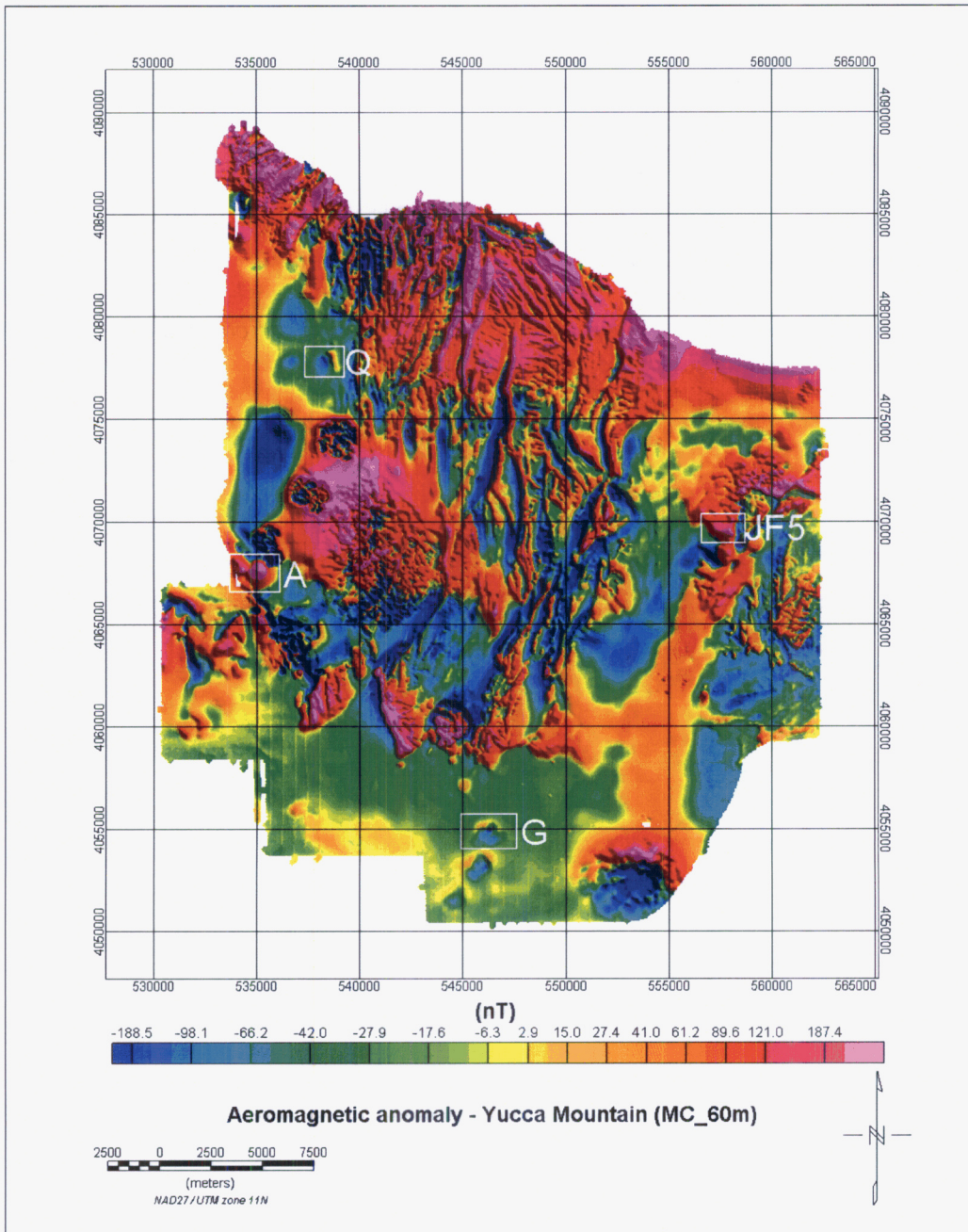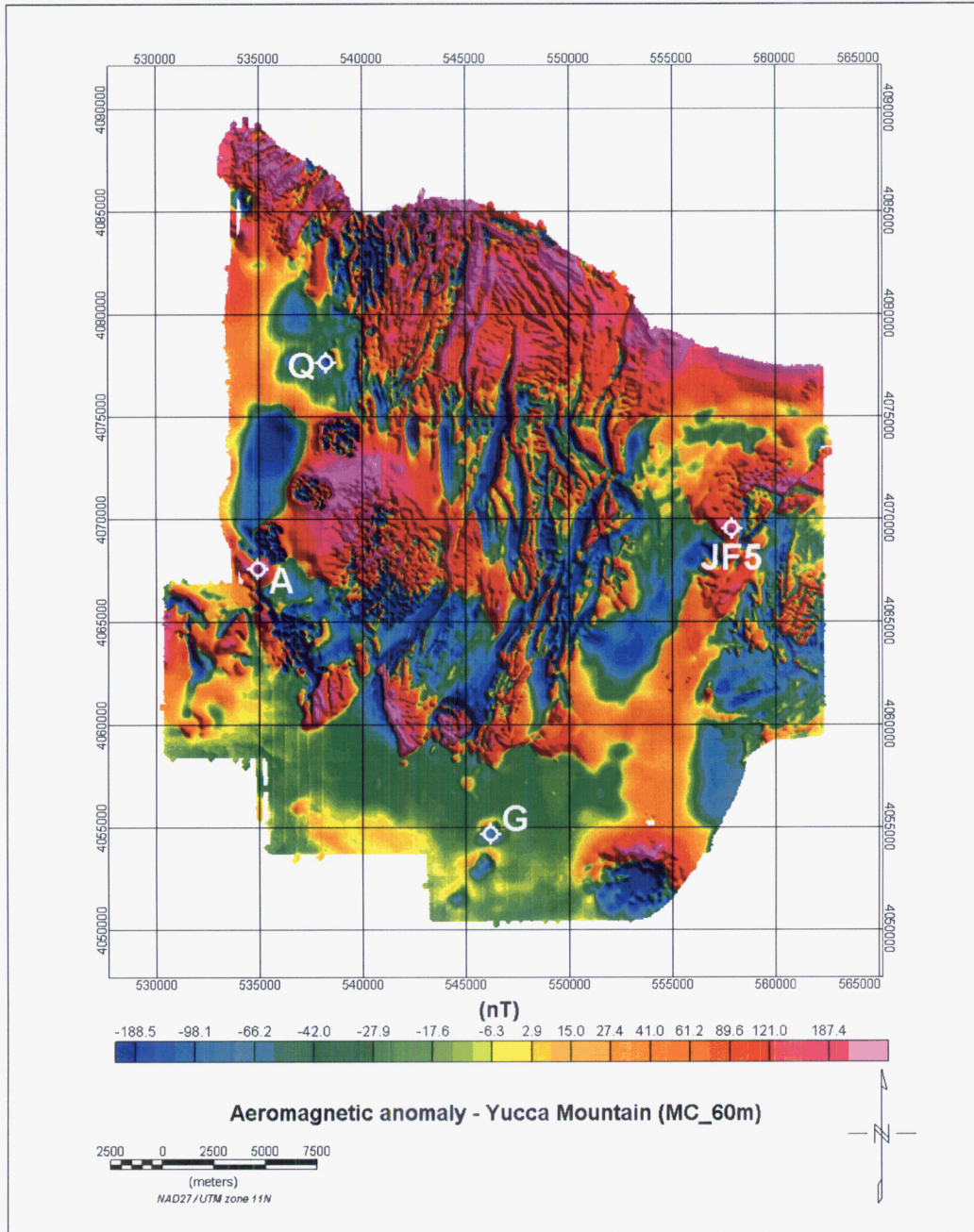**Figure 38** Total field aeromagnetic anomaly map around Yucca Mountain, Nevada compiled at approximately 30 m above the ground surface. The symbol ⋄ shows the borehole locations of anomalies A, G, JF5 and Q.

Scientific Notebook 758E

Entry: Saurav Biswas
Date: March 7, 2007
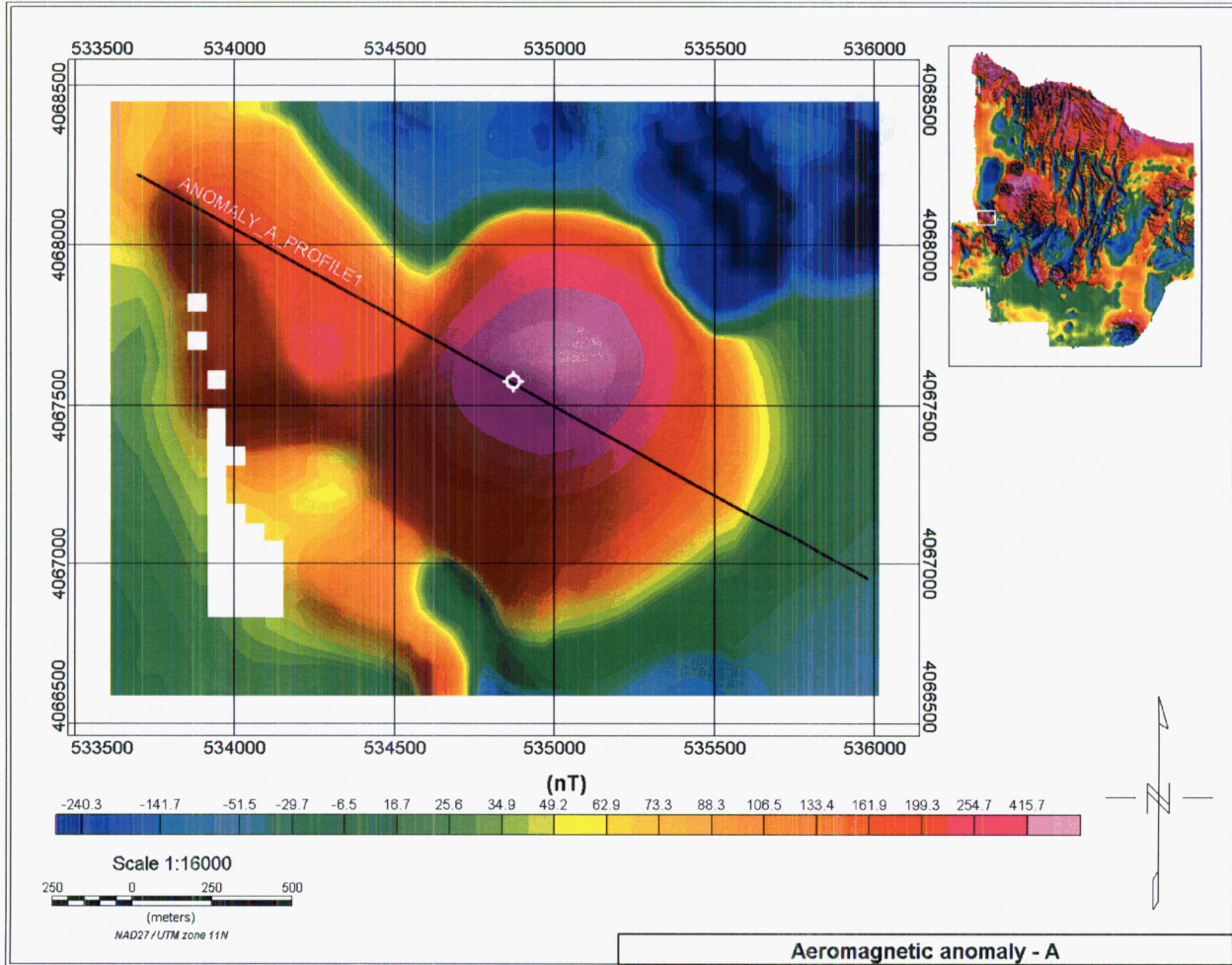
Figure 39 Total field aeromagnetic anomaly A showing the borehole location and profile location for 2-D modeling.

Entry: Saurav Biswas
Date: March 7, 2007
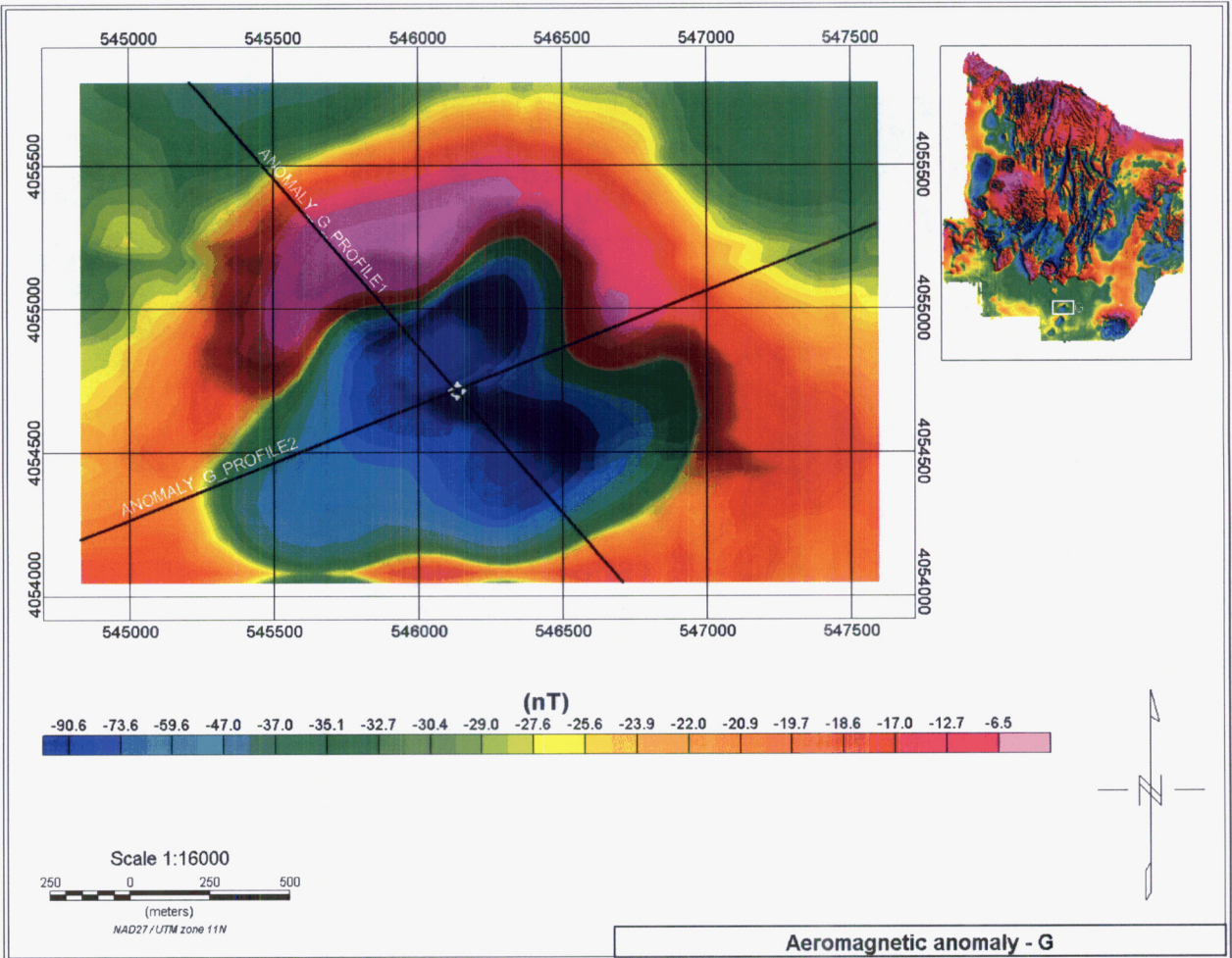
Figure 40 Total field aeromagnetic anomaly G showing the borehole location and profile locations for 2-D modeling.

Entry: Saurav Biswas
Date: March 7, 2007

Figure 41 Total field aeromagnetic anomaly JF5 showing the borehole location and profile location for 2-D modeling.

Entry:　　　Saurav Biswas
Date:　　　March 7, 2007

Figure 42 Total field aeromagnetic anomaly Q showing the borehole location and profile location for 2-D modeling.

Entry: Saurav Biswas
Date: March 7, 2007

Table 9 Source parameters for magnetic anomaly model for anomaly G

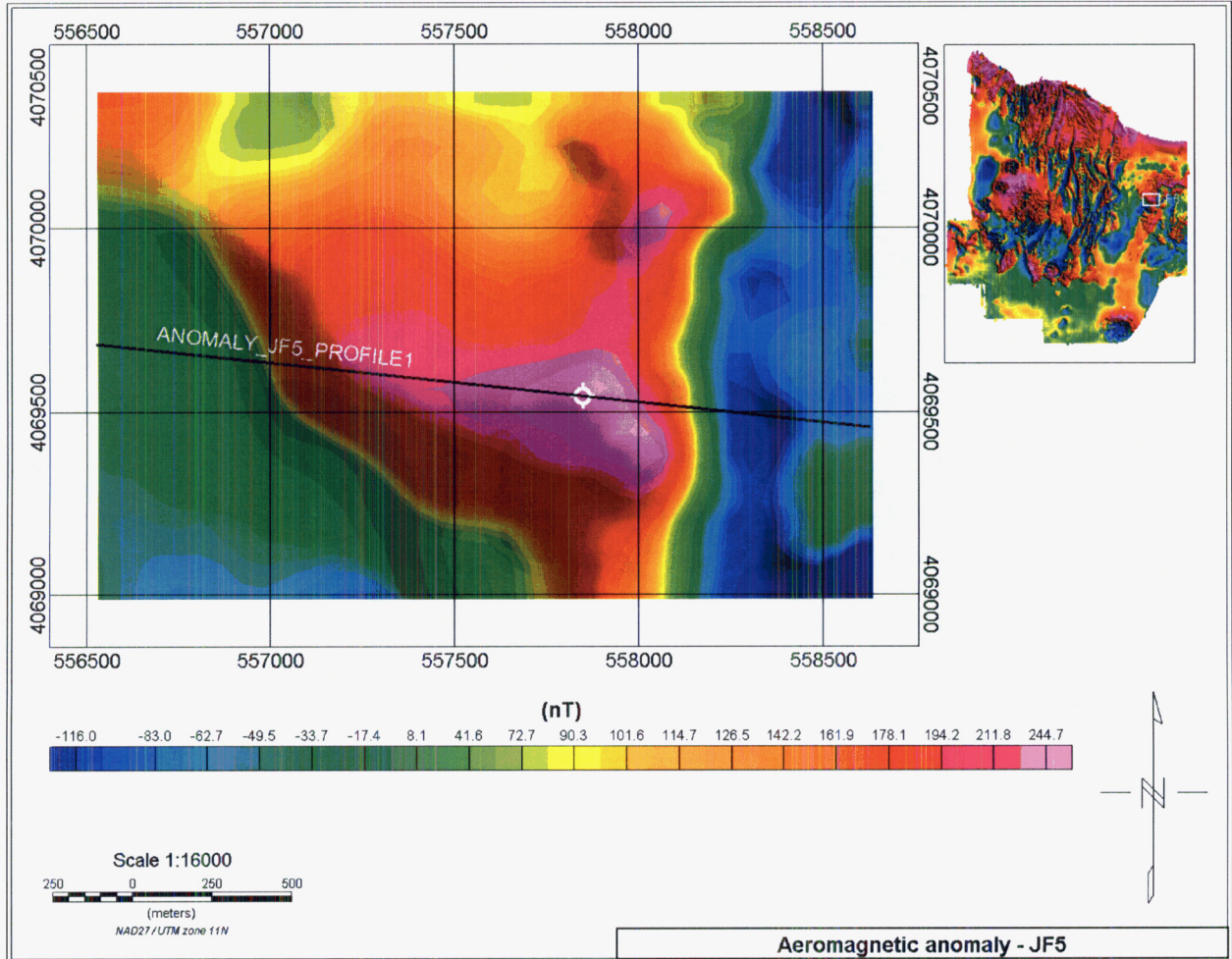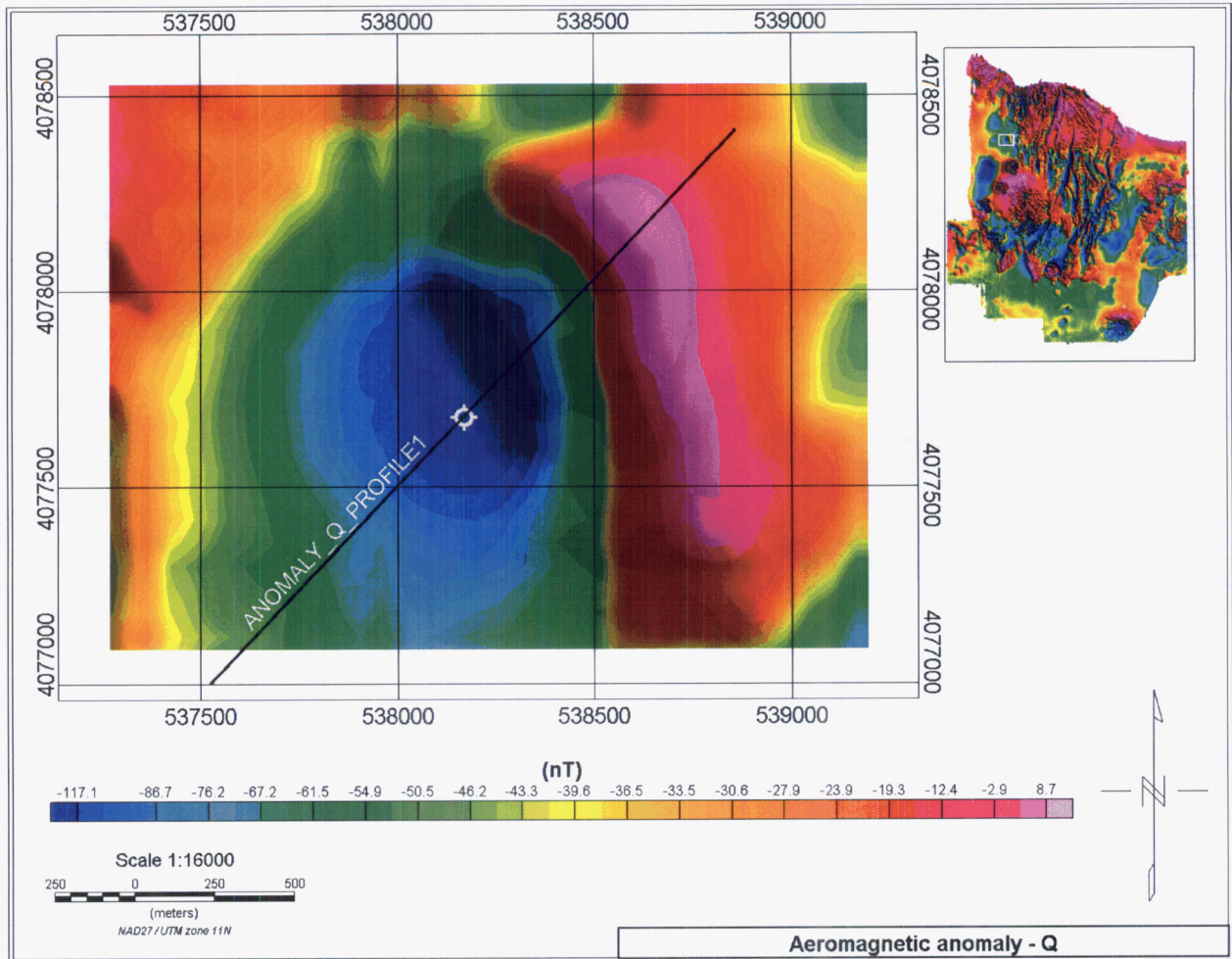| Rock Type	Susceptibility (S.I.)	Modeled Inclination	Modeled Declination	Remanent Magnetization Intensity (A/m)
Quaternary Alluvium (Qal)	0	-	-	0
Basalt	0.003	-68°	0°	1.61

Table 10 Source parameters for magnetic anomaly model for anomaly JF5

Rock Type	Susceptibility (S.I.)	Modeled Inclination	Modeled Declination	Remanent Magnetization Intensity (A/m)
Quaternary Alluvium (Qal)	0	-	-	0
Basalt	0.002	38°	0°	4.23

The magnetic parameters of the sources are based on measurements of the basalt borehole samples at Institute for Rock Magnetism (Entry 9).

Steps for modeling magnetic anomaly G profiles 1and 2 and anomaly JF5 profile1:
(1) Define the location of the anomaly G and JF5 on the total field aeromagnetic anomaly map around Yucca Mountain, Nevada – Figures 37, 40 and 41.
(2) Define profile locations for magnetic anomalies – Figures 40 and 41.
(3) Export the extracted profile data into GM-SYS for modeling – Figures 43, 44 and 45.
(4) Iteratively model the 2D subsurface geometry until the fit between observed and modeled magnetic profiles is optimized (e.g., small error).
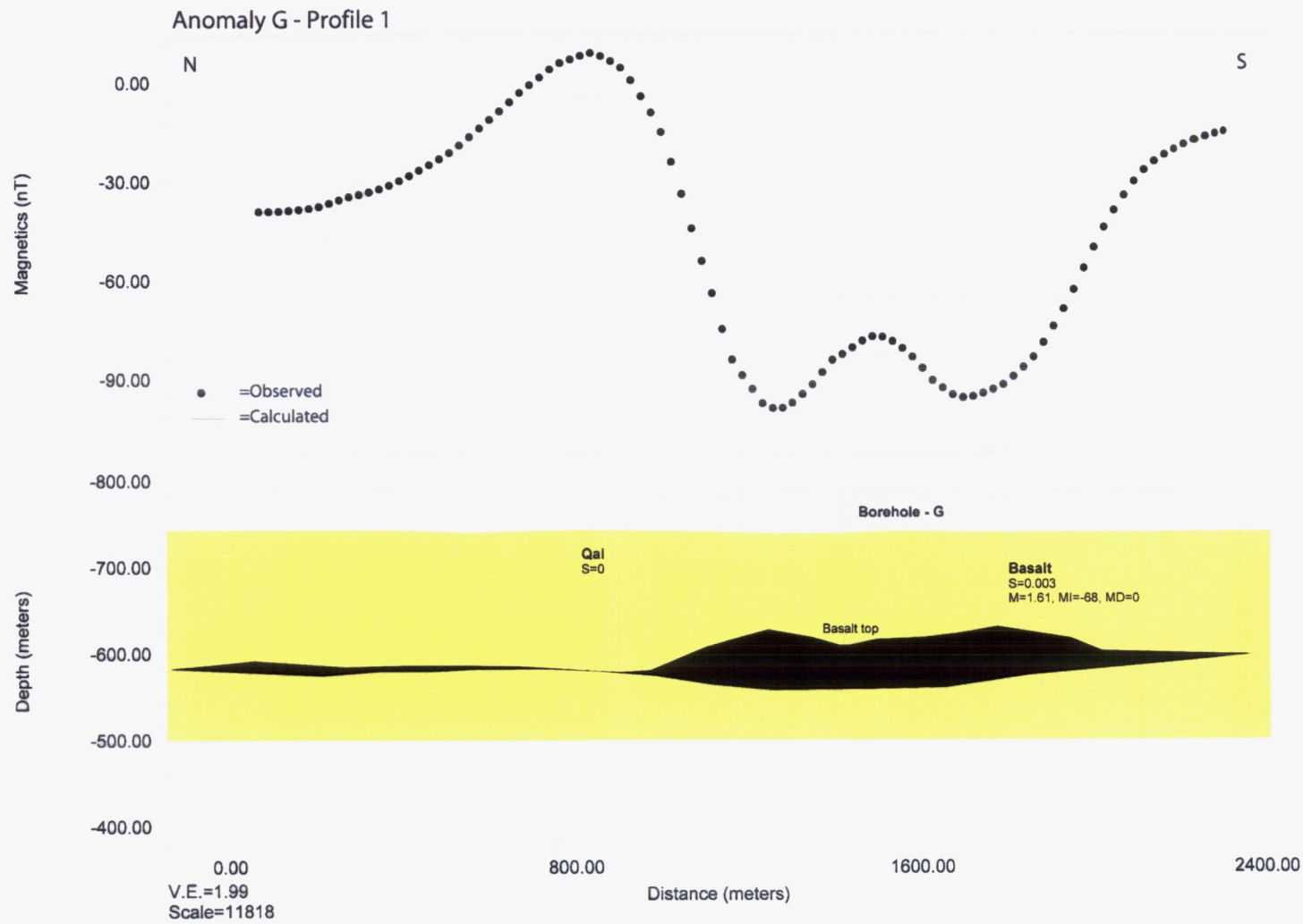
Figure 43 2D total field magnetic anomaly model for anomaly G along profile 1. Qal – Quaternary alluvium.

Anomaly G - Profile 2

Figure 44 2D total field magnetic anomaly model for anomaly G along profile 2. Qal – Quaternary alluvium.

Anomaly JF5 - Profile 1

W

E

Magnetics (nT)

300.00

200.00

100.00

0.00

-100.00

- =Observed
— =Calculated

-1000.00

-800.00

-600.00

-400.00

Depth (meters)

Borehole - JF5

Qal
S=0

Basalt top

Basalt
S=0.002
M=4.23, MI=38, MD=0

62

0.00   700.00   1400.00   2100.00
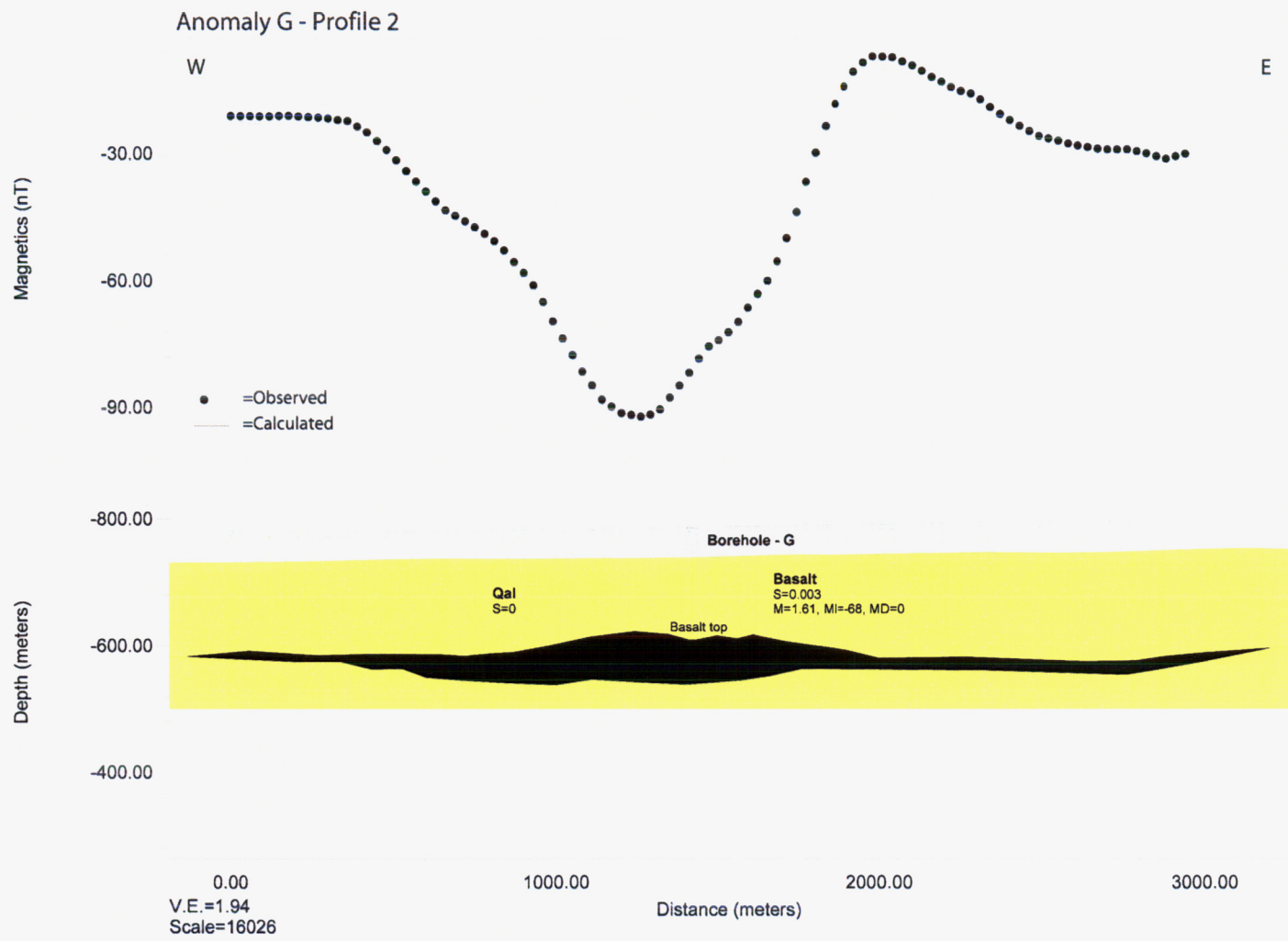V.E.=0.98
Scale=10792

Distance (meters)

Figure 45 2D total field magnetic anomaly model for anomaly JF5 along profile 1. Qal – Quaternary alluvium.
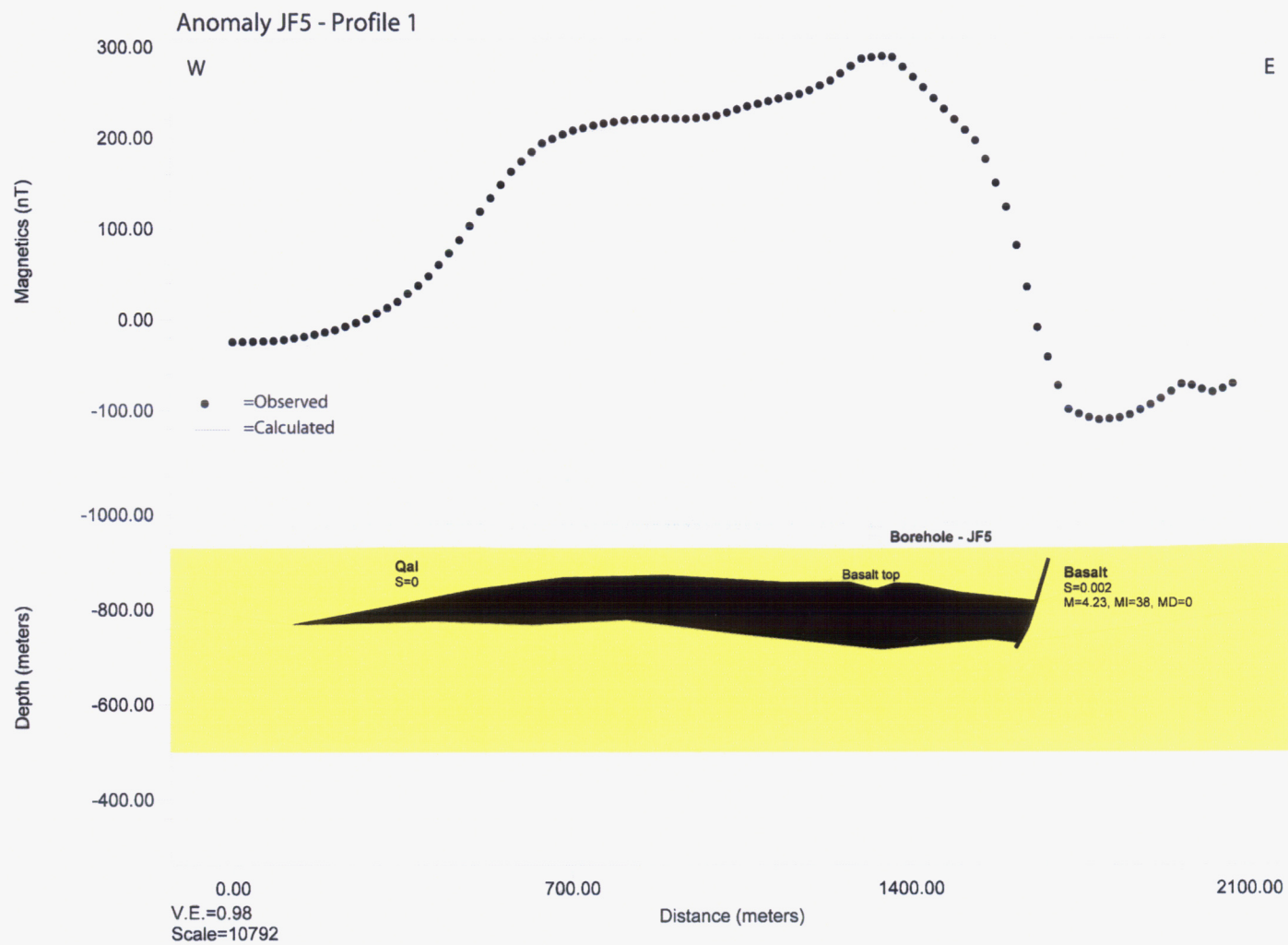
Entry: Saurav Biswas
Date: April 3, 2007

Entry 11. Revised models of anomalies Q and A incorporating new paleomagnetic data from laboratory measurements of basalts from the corresponding boreholes.

The 2D models for anomalies Q and A were revised to incorporate the new paleomagnetic data from laboratory measurements of basalts from the boreholes. The following changes were implemented:

1) Anomaly Q - The properties of remanent magnetization of basalt in Q were changed to Intensity (M) = 0.994 A/m, Modeled Inclination (MI) = -27.16°, Modeled Declination (MD) = 180° from previous values of M = 5 A/m, MI = -60°, MD = 180°. For Rainier Messa (Tmr) M was reduced to 2 A/m. M of Tmr is now consistent with range of values (0.8 – 2.7 A/m) in published literature (Brocher et al., 1998; Stamatakos et al., 2000). Pliocene basalts at shallow depth were removed. The revised model is shown in Figure 46.

2) Anomaly A - Pliocene basalt at shallow depth were removed. For Rainier Messa (Tmr) M was reduced to 2.7 A/m. M of Tmr is now consistent with range of values (0.8 – 2.7 A/m) in published literature (Brocher et al., 1998; Stamatakos et al., 2000). The revised model is shown in Figure 47. The properties of remanent magnetization of basalt in A were changed to M = 2.46 A/m, MI = 58.96°, MD = 0° from previous values of M = 20 A/m, MI = 60°, MD = 0°. The revised model is shown in Figure 48 illustrating the misfit between observed and calculated magnetic anomalies. The model was revised to match the observed magnetic anomaly. Figure 49 shows the revised model illustrating the change in source geometry of basalt. The thickness of basalt in the revised model is much larger (close to 500 m) compared to the original model (less than 100 m).

Table 11 File names of final GM-SYS 2D magnetic anomaly models

Model name	GM-SYS file name
Anomaly A – Profile 1, Original model	A_line3_oblq_1.0.6e17final.sur
Anomaly A – Profile 1, Original model with new magnetization for A	A_line3_oblq_1.0.6final_redo.sur
Anomaly A – Profile 1, Revised model	A_line3_oblq_1.2.0e17final.sur
Anomaly G – Profile 1	Aeromag_G_profile1_2layer1.0.4e6_final.sur
Anomaly G – Profile 2	Aeromag_G_profile2_2layer1.0.5e2_final.sur
Anomaly JF5 – Profile 1	Aeromag_JF5_profile1_2layer1.0.3e28_final.sur
Anomaly Q – Profile 1	Q_oblique_line2_model05_Layer_basalt09.1e4_final.sur

Earth's magnetic field parameters for all the above models during the survey period:
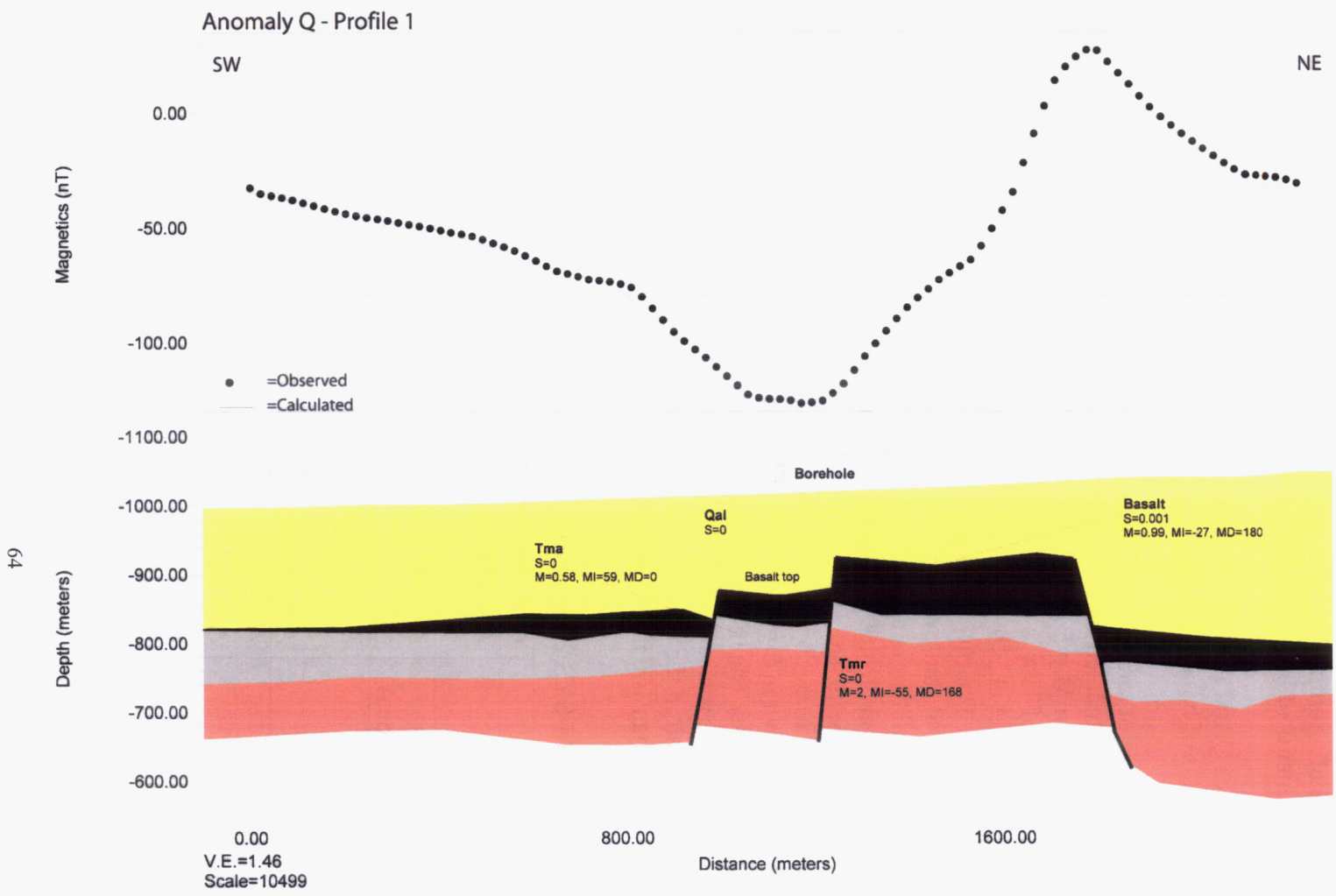Magnitude, H = 39.8 A/m (50,000 nT) Inclination = 60° and Declination = 14°.

Figure 46 2D model for anomaly Q along profile 1. Qal – Quaternary alluvium, Tma – Ammonia Tanks, Tmr – Rainier Mesa.
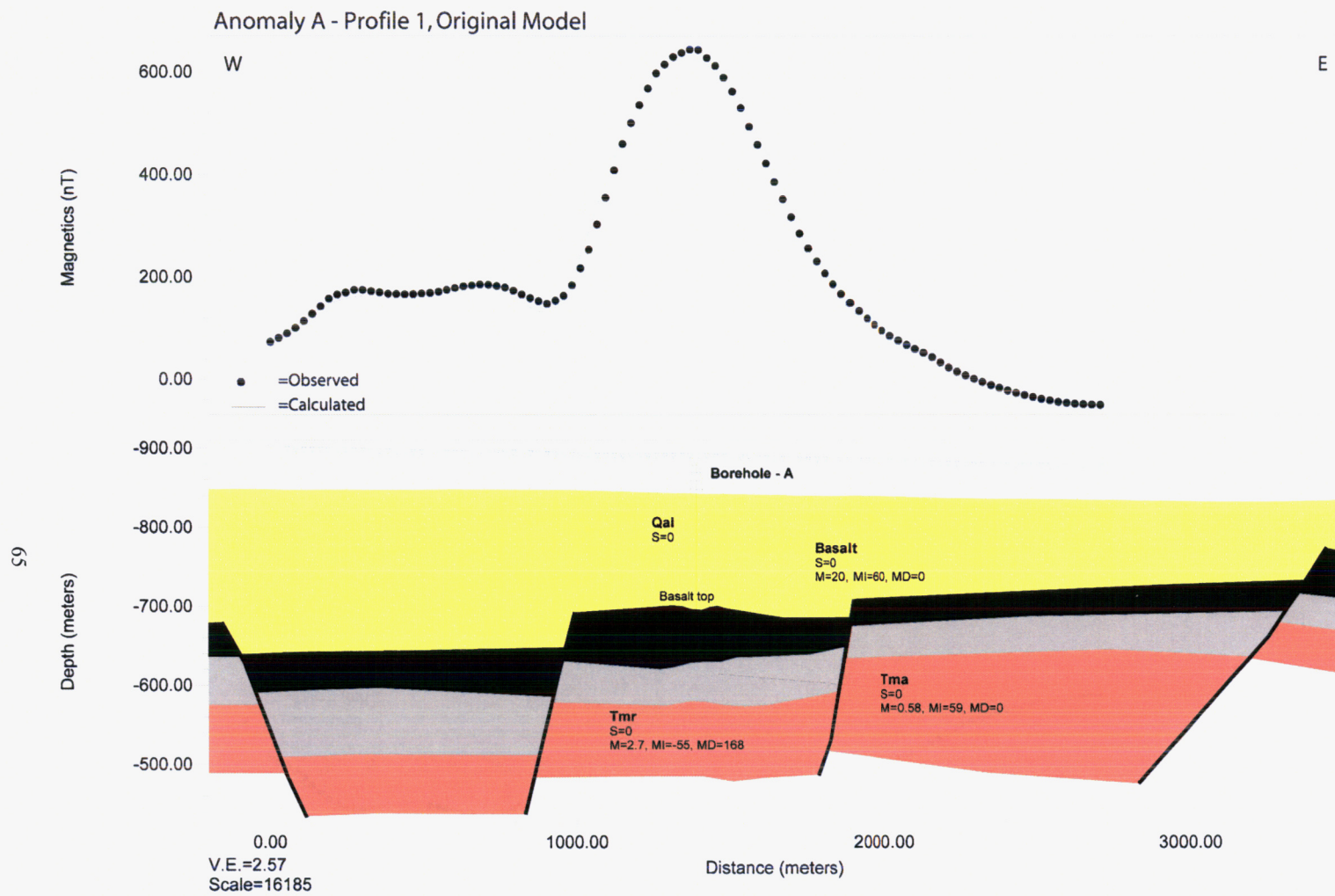
64

Figure 47 Original 2D model of anomaly A along profile 1 prior to laboratory measurements of paleomagnetic properties of basalt samples from anomaly A borehole. Qal – Quaternary alluvium, Tma – Ammonia Tanks, Tmr – Rainier Mesa.
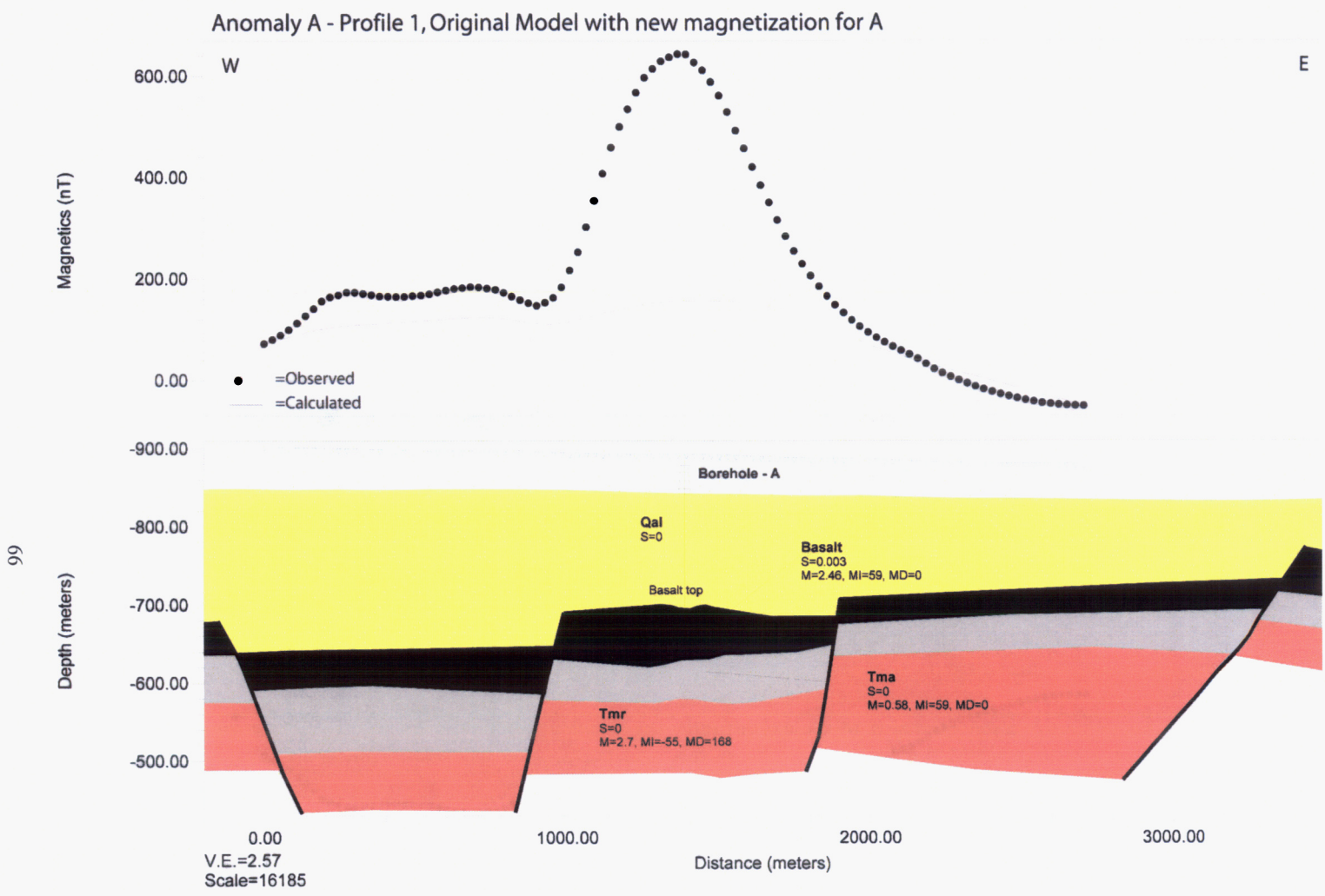
Figure 48 Original 2D model of anomaly A along profile 1 with new intensity of basalt showing the misfit between observed and calculated anomaly. Qal – Quaternary alluvium, Tma – Ammonia Tanks, Tmr – Rainier Mesa.

Saurav Biswas
April 3, 2007

Anomaly A - Profile 1, Revised Model
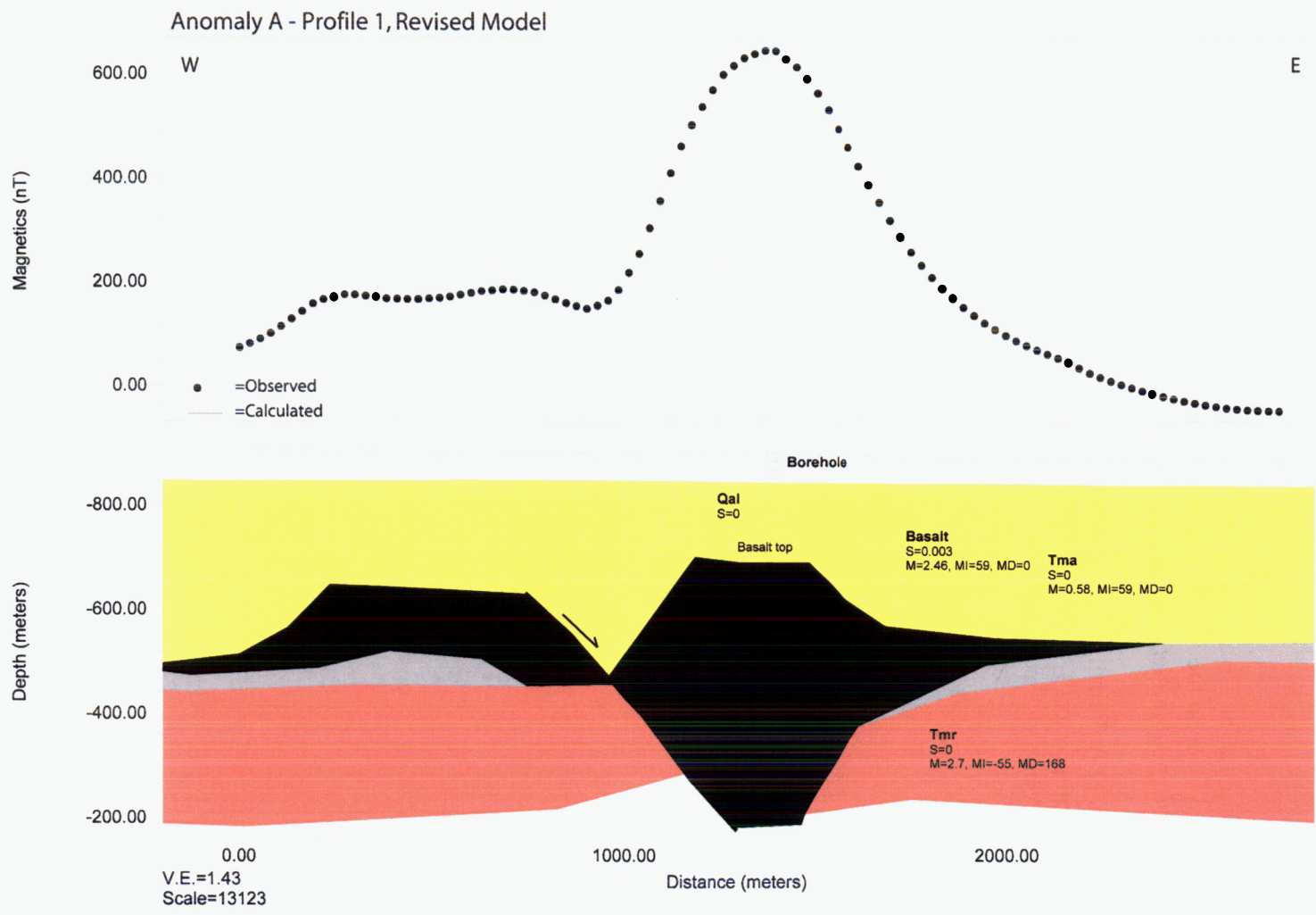
Figure 49 Revised 2D model of anomaly A along profile 1 with new intensity of basalt. Qal – Quaternary alluvium, Tma – Ammonia Tanks, Tmr – Rainier Mesa.

Scientific Notebook 758E

67

Scientific Notebook 758E

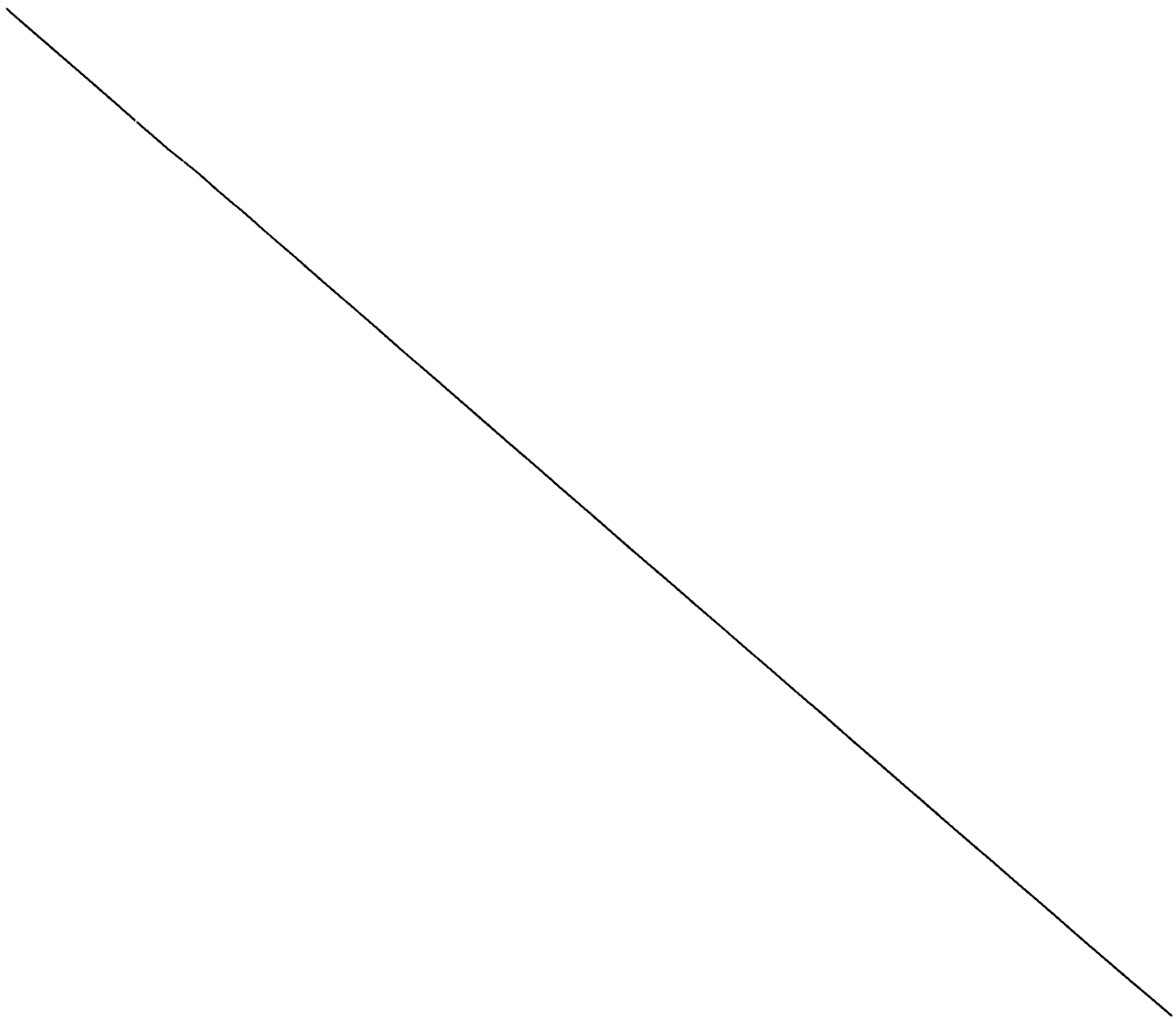**Entry:** Saurav Biswas
Date: April 3, 2007

Reference:

Brocher, T.M., and W.C. Hunter, and V.E. Langenheim. "Implications of seismic Reflectionand Potential Field Geophysical Data on the Structural Framework of the Yucca Mountain-Crater Flat Region, Nevada." *Geological Society of America Bulletin.* Vol. 110. pp. 947-971. 1998.

Stamatakos, J.A., B.E. Hill, D.A. Ferrill, P.C. LaFemina, D. Sims, C.B. Connor, M.B. Gray, A.P. Morris, and C.M. Hall. "Composite 13-Ma Record of Extensional faulting and Basin Growth of Crater Flat, Nevada." San Antonio, Texas: CNWRA. 2000.
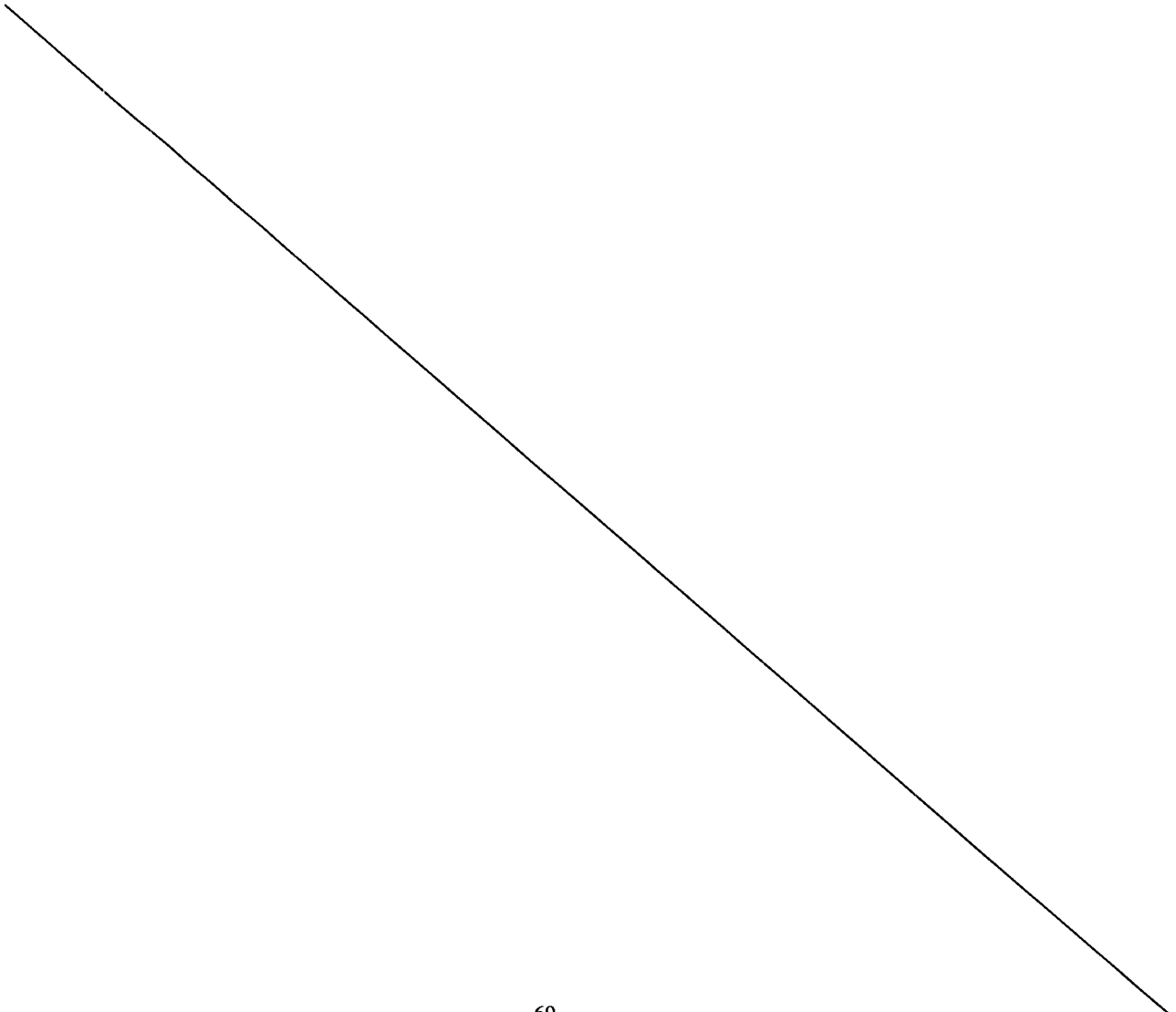
Entry: Saurav Biswas
Date: April 4, 2007

Entry 12. Revised maps of the entire helicopter survey region and anomalies A, G, JF-5 and Q to show different colour scheme and colour scale bar with uniform interval.

All the previous magnetic anomaly maps in the entire helicopter survey region by DOE in 2004 were plotted with a red-blue colour scheme (Figure 50 - 54) to distinguish them from rainbow colour scheme used in the magnetic anomaly maps made available by DOE. The new maps show colour bar with uniform interval. A new magnetic anomaly map was plotted (Figure 55) showing the locations of all the anomalies in this region. This illustrates the spatial clustering of multiple anomalies.

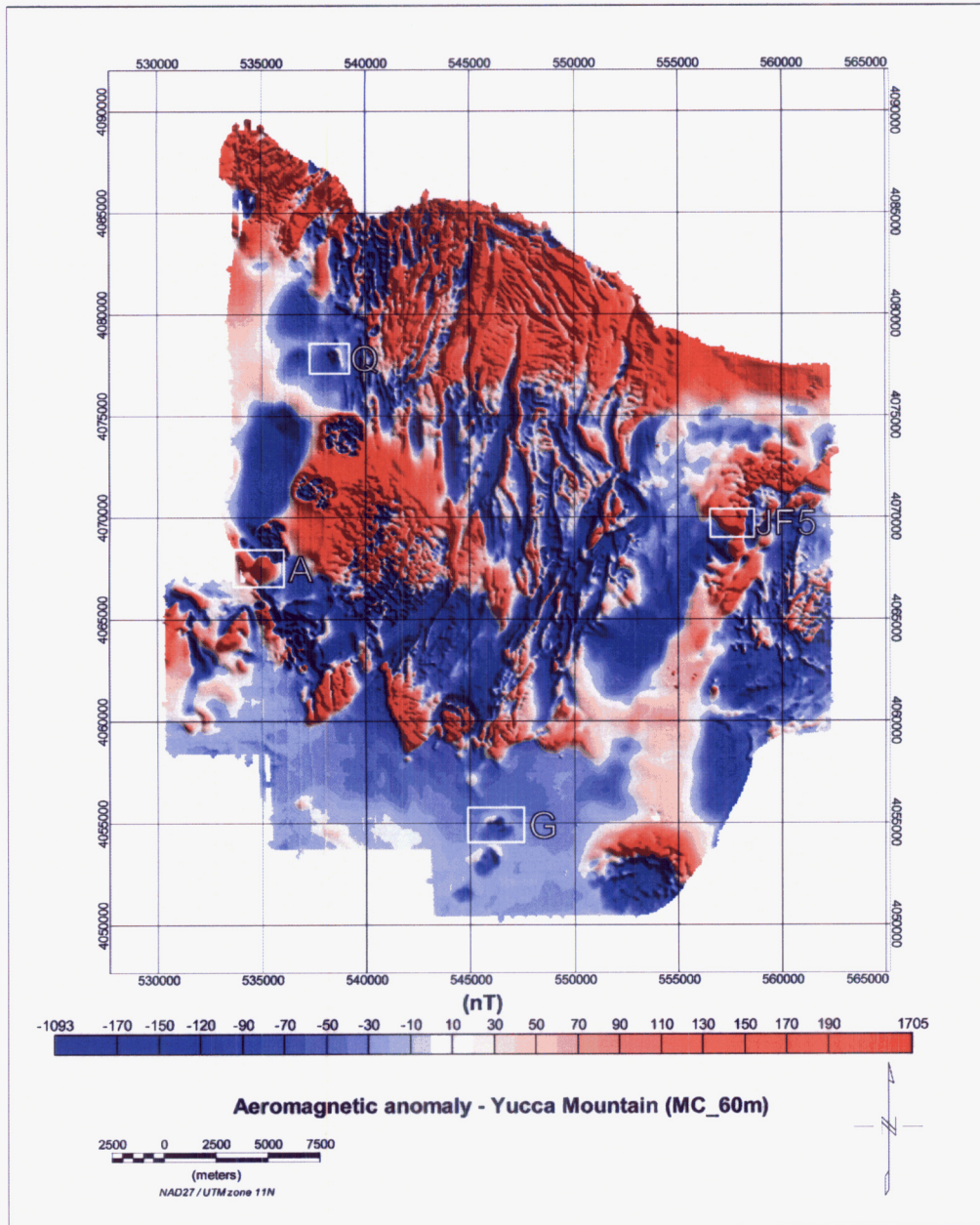**Entry:**   Saurav Biswas
Date: April 4, 2007

Figure 50 Total field aeromagnetic anomaly map around Yucca Mountain, Nevada compiled at approximately 30 m above the ground surface. The white rectangles show the anomalies A, G, JF5 and Q.

Entry: Saurav Biswas

Date: April 4, 2007

Figure 51 Total field aeromagnetic anomaly A showing the borehole location and profile location for 2-D modeling.

Entry: Saurav Biswas
Date: April 4, 2007

Figure 52 Total field aeromagnetic anomaly G showing the borehole location and profile locations for 2-D modeling.

Entry: Saurav Biswas
Date: April 4, 2007

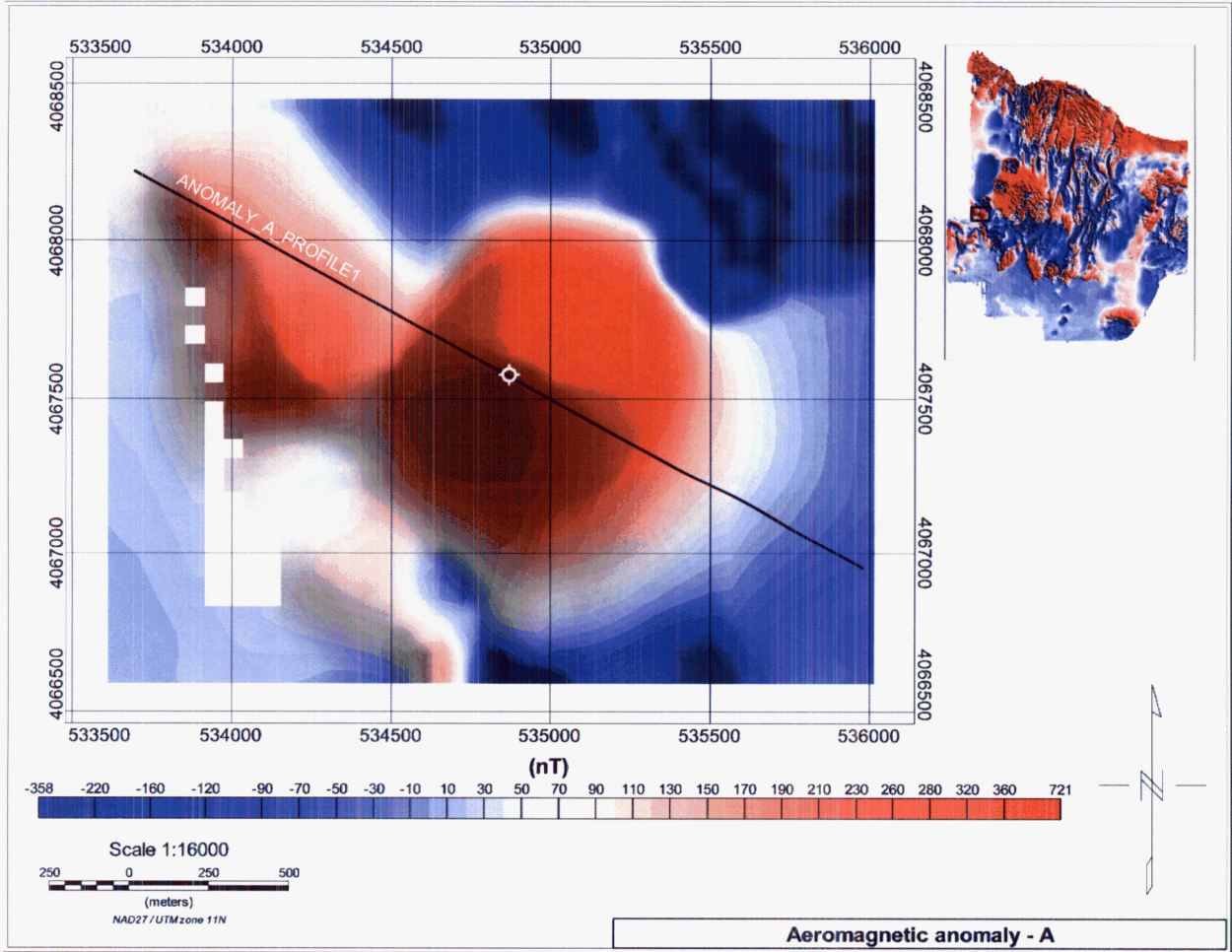**Figure 53** Total field aeromagnetic anomaly JF5 showing the borehole location and profile location for 2-D modeling.

Entry: Saurav Biswas
Date: April 4, 2007

Figure 54 Total field aeromagnetic anomaly Q showing the borehole location and profile location for 2-D modeling.
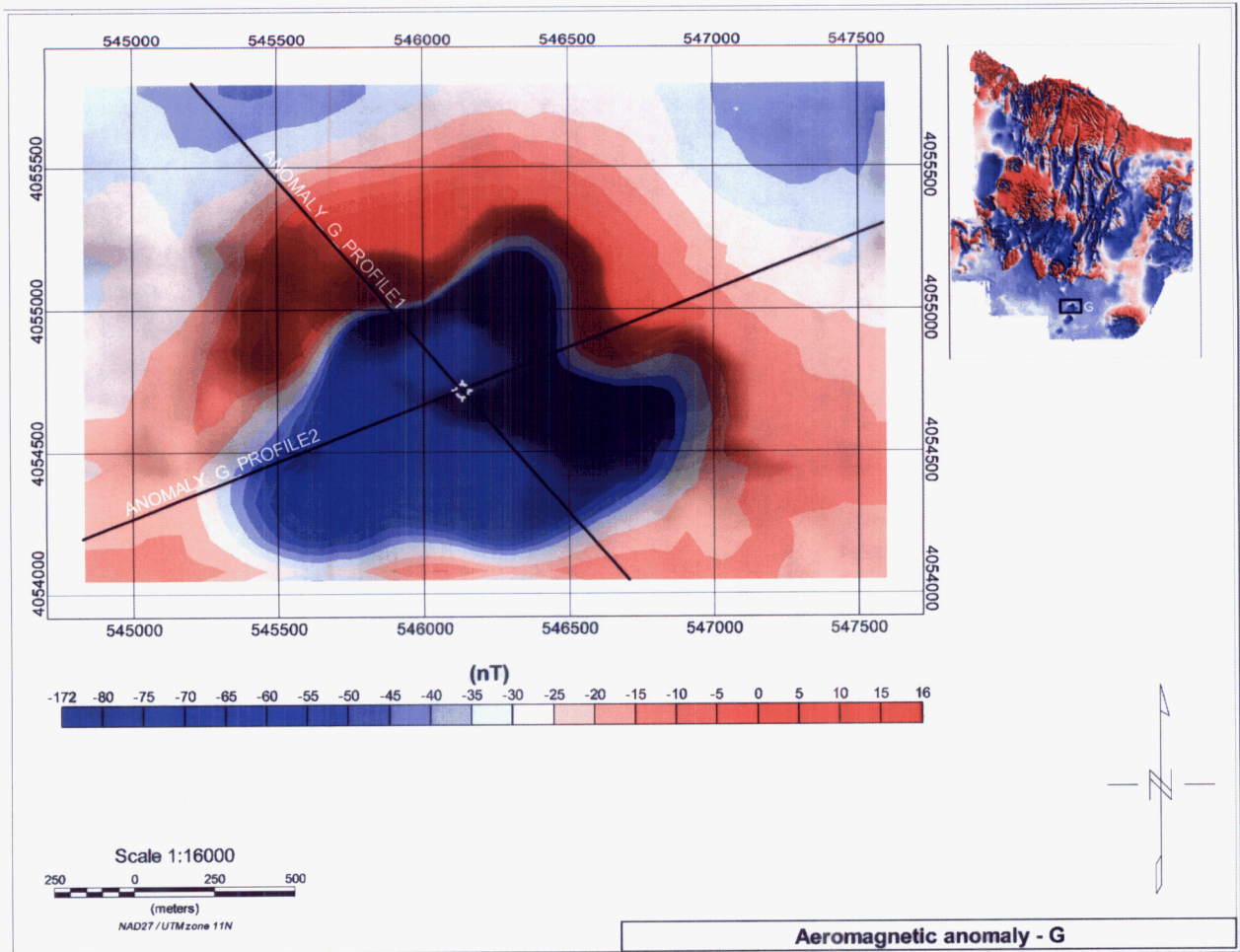
Entry: Saurav Biswas
Date: April 4, 2007

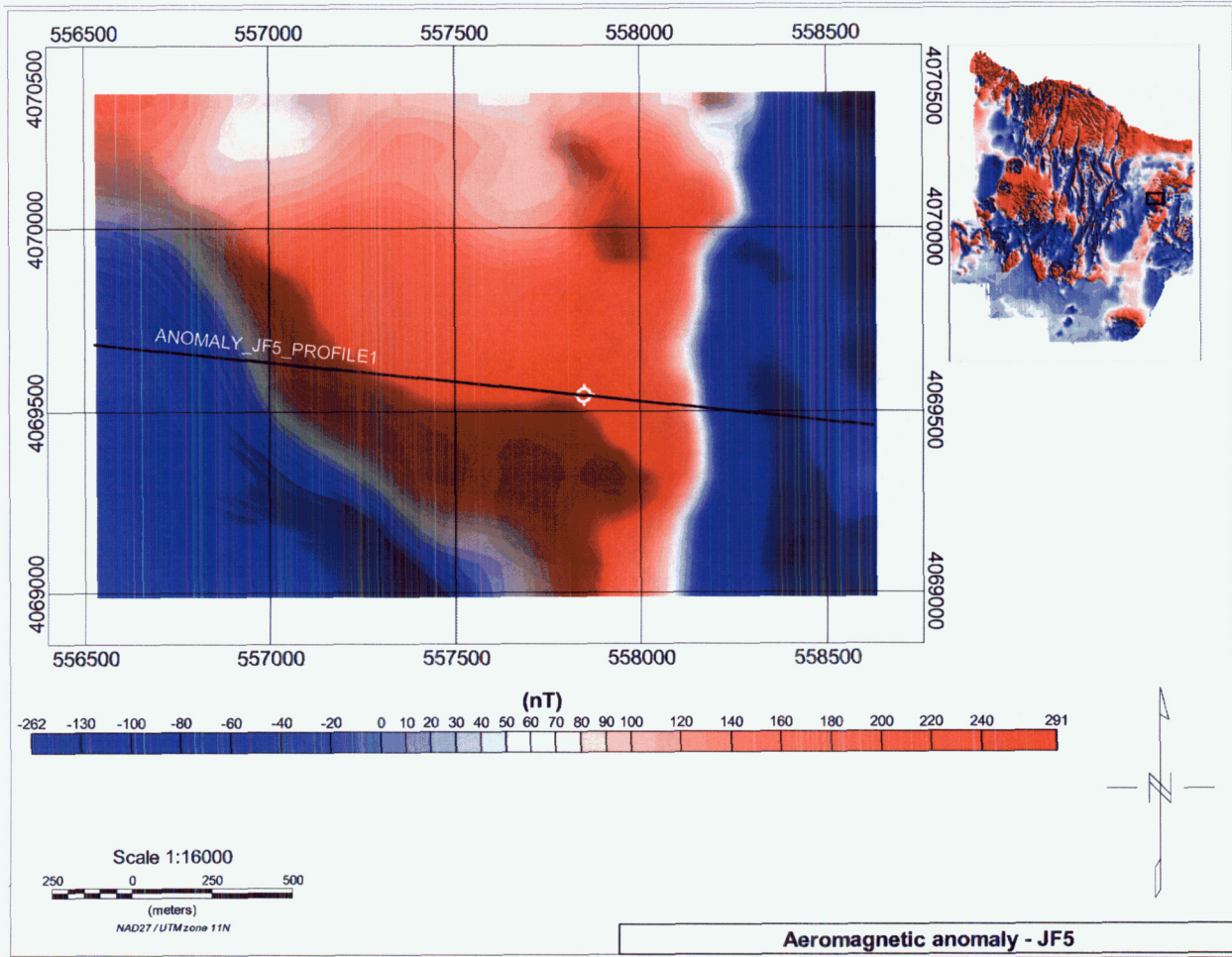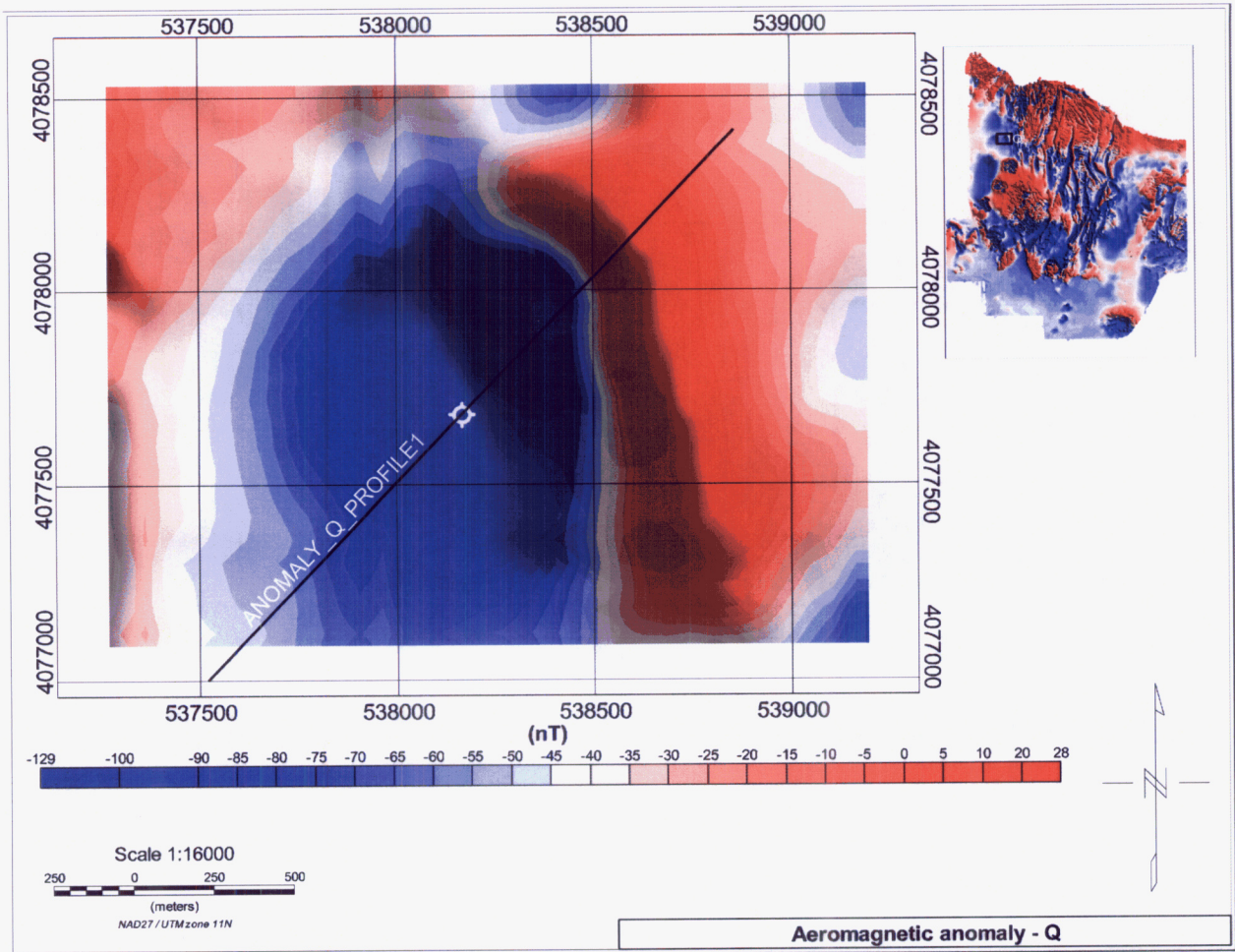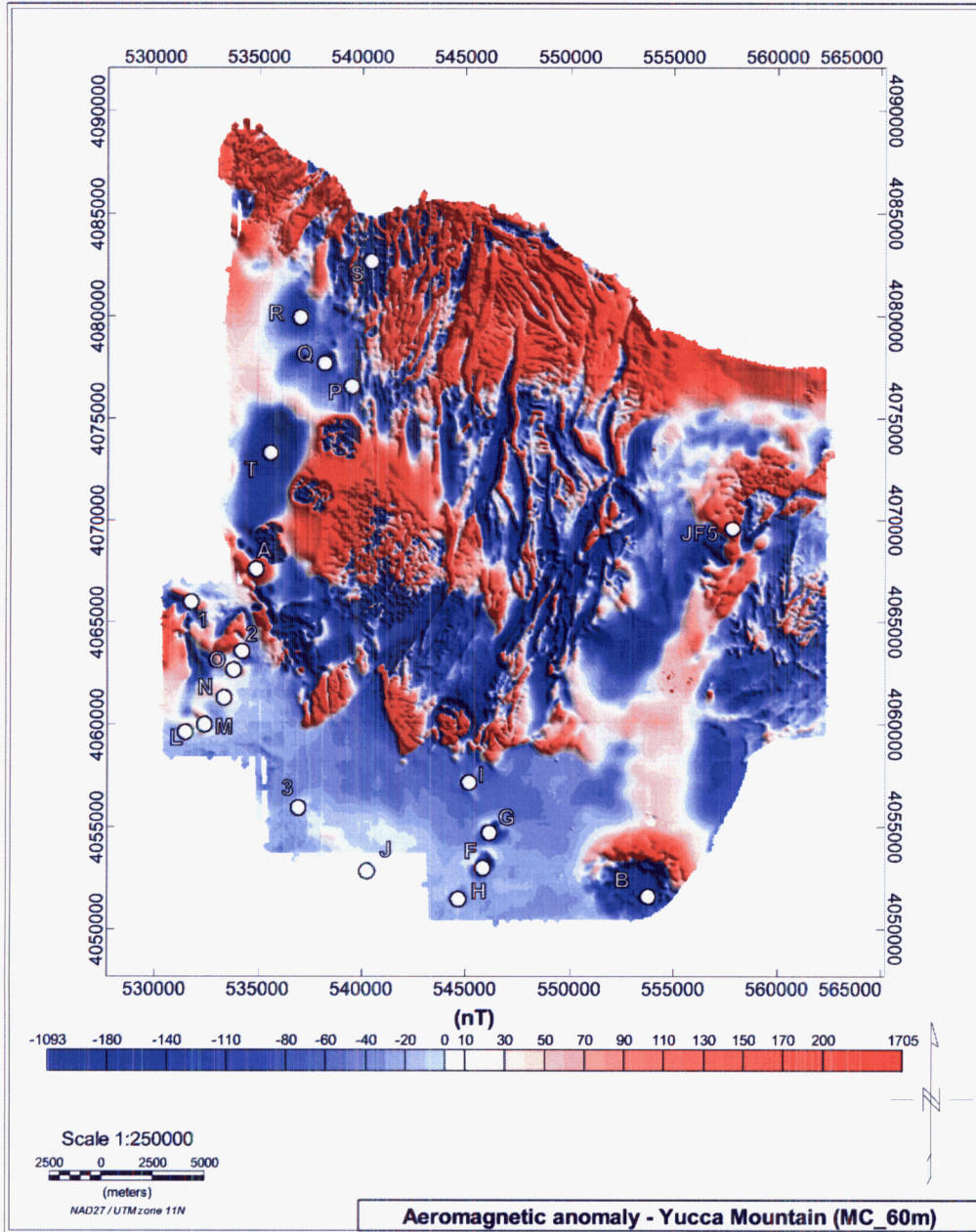**Figure 55** Total field aeromagnetic anomaly map around Yucca Mountain, Nevada compiled at approximately 30 m above the ground surface showing all the anomalies in the region.

Entry:	Saurav Biswas
Date:	April 6, 2007

Entry 13. Installation testing of Oasis montaj ^{TM} 6.3.1 (Geosoft 2006).

It was noted that the current version of Oasis montaj 6.3.1 (Geosoft 2006) was not included in the software control list. An installation test was performed to include the current version of Oasis montaj in the software control list.

All the files required for installation testing are located at
D:\Oasis_montaj\Oasis_6.3.1_6G\Test_Directory. Data from software validation test of Oasis montaj Version 5.1.8 (Winfrey, 2003) were used to perform the installation test. The output map (Figure 56) was identical with the map documented in the software validation test by Winfrey (2003).

The installation test was successful and a software release notice has been signed. The validation for the software will be completed within 60 days.

Entry: Saurav Biswas
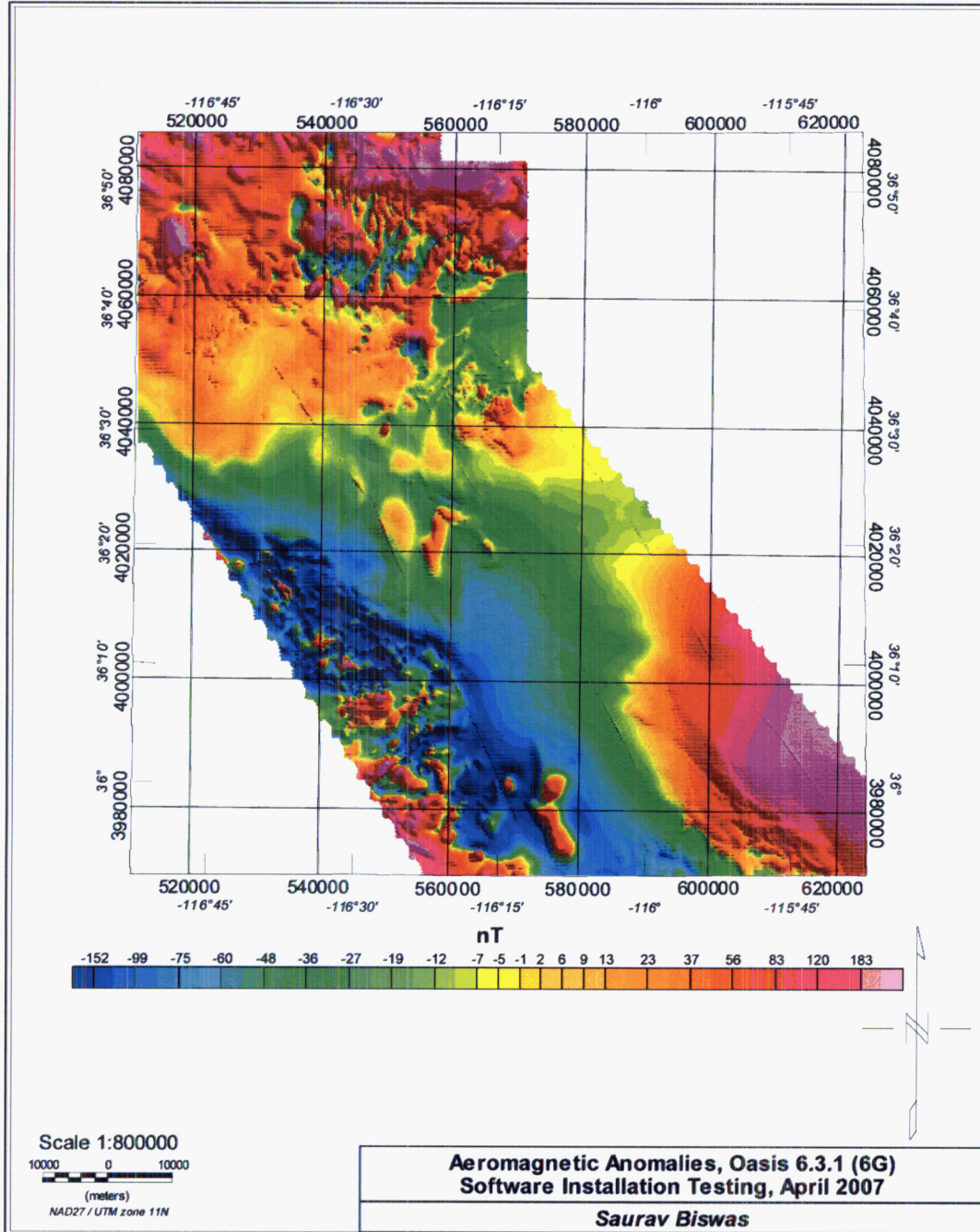**Date:**   April 6, 2007

Figure 56 Final aeromagnetic anomaly map prepared during software installation testing.

Scientific Notebook 758E

Entry: Saurav Biswas
Date: April 6, 2007

Reference:

Winfrey, B. "Software Validation Test Plan and Report Oasis montaj [TM], Version 5.1.8" San Antonio, Texas: CNWRA. 2003.

Scientific Notebook 758E

Entry: Saurav Biswas
Date: February 21, 2008

Entry 14. Completion of validation of Oasis montaj ™ 6.3.1 (Geosoft 2006).

Software validation for Oasis montaj ™ 6.3.1 was completed in January 2008 and the process is documented in the report by Biswas (2008). Oasis montaj ™ 6.3.1 is currently listed as validated software in the Controlled Software List in ELF.

This concludes all the entries in this scientific notebook.

Reference:

Biswas, S. "Software Validation Test Plan and Report Oasis montaj ™, Version 6.3.1" San Antonio, Texas: CNWRA. 2008.

ADDITIONAL INFORMATION FOR SCIENTIFIC NOTEBOOK NO. 758E

Document Date:	02/08/2006
Availability:	Southwest Research Institute® Center for Nuclear Waste Regulatory Analyses 6220 Culebra Road San Antonio, Texas 78228
Contact:	Southwest Research Institute® Center for Nuclear Waste Regulatory Analyses 6220 Culebra Road San Antonio, TX 78228-5166 Attn.: Director of Administration 210.522.5054
Data Sensitivity:	■"Non-Sensitive" ☐ Sensitive ☐"Non-Sensitive - Copyright" ☐ Sensitive - Copyright
Date Generated:	10/01/2006
Operating System: (including version number)	Windows
Application Used: (including version number)	WordPerfect 10, SLIM
Media Type: (CDs, 3 1/2, 5 1/4 disks, etc.)	1 DVD
File Types: (.exe, .bat, .zip, etc.)	Oasis montaj© Version 5.1.8(A5) (Geosoft, 2000) and Version 6.3.1 (6G) (Geosoft 2006), GM-SYS© (Geosoft) 4.8.45b (Northwest Geophysical Assoc., 2001). Microsoft ® Excel 2002 (10.6501.6735) SP3, Copyright © Microsoft Corporation 1985-2001. IAPD 2000
Remarks: (computer runs, etc.)	Media contains: